

**DEVELOPMENT AND EVALUATION OF NANO-HERBAL
THERAPY FOR METASTATIC BREAST
CANCER TREATMENT**

A Dissertation
Submitted to
the Temple University Graduate Board

In Partial Fulfillment
of the Requirements for the Degree
DOCTOR OF PHILOSOPHY

by
Wucheng Wen
December 2018

Examining Committee Members:

Dr. Ho-Lun Wong, Thesis Advisor, School of Pharmacy
Dr. Benjamin E. Blass, TU School of Pharmacy
Dr. Reza Fassihi, TU School of Pharmacy
Dr. Thomas Dürig, External member, Ashland Specialty Ingredients

©
Copyright
2018

by

Wucheng Wen
All Rights Reserved

ABSTRACT

Triptolide (TPL), a diterpenoid triepoxide that is extracted from a traditional Chinese herb called *Tripterygium Wilfordii* (also known as ‘Thunder God Vine’) has recently drawn increasing interests from pharmaceutical and biomedical researchers, especially in the aspect of its potential efficacy on multiple cancer treatment. TPL has shown significant growth and proliferation inhibition activities in a broad range of cancer cell types. Moreover, it has shown the inhibition of osteoclastogenesis by breast cancer bone metastasis. However, due to its limitation in toxicity, solubility and non-specific biodistribution, it is challenging for the application of TPL in clinical study. On the other hand, TPL can rapidly distribute in most vital organs and no evidences shown tissue accumulation of drug. It is important to overcome those barriers and optimize the properties and performance of the promising drug molecule.

Lipid-based nanocarriers such as nanostructured lipid carriers (NLC) have been extensively studied for delivery of poorly-water soluble drug compounds. They also have the potential to optimize the physicochemical properties of the drug and may enhance a targeted delivery of the drug to specific therapeutic site. Alendronate (Fosamax®), an FDA approved bisphosphonate drug for osteoporosis, osteogenesis imperfecta and several other bone diseases, has been used as a bone targeting decoration agent. Breast cancer cell line MDA-MB-231 and other type of cancer cell lines have been used to study the *in vitro* cytotoxicity of TPL and the carriers while MC3T3-E1 cell line was used for toxicity assessment.

After modifying and optimizing the formulation of the particle, the formulation had the ability to remain structurally and functionally stable when in bio-simulated media at 37 °C and in water at room temperature with high encapsulation efficiency. *In vitro* study illustrated that both TPL free drug (stock solution 10mg/mL dissolved in DMSO) and TPL nanoparticle without alendronate (TPL-NP) had similar cytotoxicity on MDA-MB-231 and some other type of cancer cell lines. The ALE decoration on the particle (ALE-NP-TPL) has enhanced the anti-cancer effect especially with breast cancer cell line. The *ex vivo* study shows that after incubation of ALE-NP formulation with bone tissues, the formulation and TPL showed strong binding signal on the bone compared with free drug. TPL-NP has not only successfully optimized the physicochemical properties of the drug, but also shows significant enhancement of therapeutic effect both *in vitro* and *ex vivo* study.

This thesis work is dedicated to my parents Xin Wen and Shiman Wu and my wife Dr.
Zheng Lu for endless love and supports.

ACKNOWLEDGMENTS

This thesis was done with tremendous effort not only from the author, but also with great help and supports from many people. I would like to thank my supervisor, Dr. Ho-lun Wong, without whom I will never learn so much on the path of novel drug delivery system and cancer research. Dr. Wong not only help me with my thesis and difficulties, but always stand by me and support me. It's my honor to have such a great professor during my PhD study and research.

I would like to express my special thanks of gratitude to my committee members Dr. Benjamin Blass, Dr. Daniel Canney and Dr. Reza Fassihi who provide valuable advices and suggestions for my project. Only with those help can I stay in the right track and focus on the final goal of the project. They not only taught me the way of thinking and studying for PhD, but also the knowledge of life that will benefit me much longer in my life.

What's more, I really appreciate Dr. Thomas Dürig, Dr. Vivian Bi and Dr. Nick Chen from Ashland Specialty Ingredients who supported me and helped me during my working in the company. Especially thanks to Dr. Dürig who not only guided and helped me through my scientific journey, but also be my external committee member with tight schedule. It's my honor to have Dr. Dürig on my committee panel.

I also appreciate Dr. Hui-Yi (Joanne) Xue who train me from scratch and guide me through my research, especially during *in vitro* cell work and *in vivo* animal study. Dr. Xue was extremely patient and supportive when I just joined the lab and push me onto the right track of PhD research study. Ngoc Tran also worked with me along the

road. She also trained me with various experiments and showed expertise during my research.

Pengbo Guo, Di Wu, June Young Eoh, Mengjie Si, Mariam Botros and Zhongling Li, who are or were the colleagues from my lab, provided me help and supports along my road. Especially Pengbo who showed creative thinking and ability to help with my project that played indispensable role during my PhD degree.

A lot of people from school of pharmacy also played important role in this project. Min Ye and Dr. John Gordon guided me and provided me patient help during my animal study. Dr. Marc Ilies kindly share with me the equipment in his lab. Kimberly Holt provided me with supportive idea and suggestions.

Last but not least, I would like to express my special thanks to my beloved family. Without my parents supports, I can never accomplish this achievement far away from home. It's their love and supports and motivate me to overcome the difficulties. Dr. Zheng Lu not only provides me accompany and love, but also gives me great idea for my project along my PhD study. It's my luck to marry such extraordinary woman during my time in Temple University. I would also like to thank my beloved fur friend Leon and Tony who also stay with me when there's difficulties or accomplishment.

TABLE OF CONTENTS

	Page
ABSTRACT.....	iii
DEDICATION.....	v
ACKNOWLEDGMENTS	vi
LIST OF TABLES.....	xii
LIST OF FIGURES	xiii
CHAPTER	
1. BONE METASTATIC BREAST CANCER	1
1.1. Introduction	1
1.2. Mechanism and Rational	5
1.2.1. Metastatic Breast Cancer	5
1.2.1.1. Various Types of Breast Cancer	5
1.2.1.2. Mechanism of MBC	7
1.2.1.3. Bone Metastasis	8
1.2.2. Current Treatment and obstacles	12
2. TRIPTOLIDE	17
2.1. Introduction	17
2.2. Anti-cancer Effect	22
2.3. Osteoclast Inhibition	29
2.4. Current Obstacles of Triptolide	31
3. BONE TARGETING NANOPARTICLES.....	37

3.1. Nano-Structure Lipid Carrier	37
3.1.1. Introduction	37
3.1.2. Solubility Enhancement	39
3.1.3. Preparation	40
3.2. Alendronate	42
3.2.1. Introduction	42
3.2.2. Mechanism of Bone Targeting	44
3.2.3. Preparation of ALE conjugated phospholipid	44
3.3. Particle Characterization Techniques	46
3.3.1. Preparation Size Distribution and Surface Charge	46
3.3.2. Encapsulation Efficiency (EE)	47
3.3.3. Morphology	48
3.3.4. Cytotoxicity Study	49
3.3.5. Stability	51
4. OBJECTIVES OF THE STUDY	52
5. EXPERIMENTAL SECTION	53
5.1. Materials	53
5.2. Preparation of Triptolide Nanoparticle (TPL-NP)	54
5.3. Preparation of Alendronate Conjugated Phospholipid	56
5.4. Preparation of Alendronate Decorated Triptolide Nanoparticle	57
5.5. Characterization of TPL-NP	58
5.5.1. Particle Size Distribution and Surface Charge	58
5.5.2. Stability	59

5.5.3. Encapsulation Efficiency (EE)	60
5.5.4. Hydroxyapatite Affinity Study	61
5.5.5. Drug Releasing Study	62
5.5.6. Morphology	62
5.5.7. Cytotoxicity Study	64
5.5.8. Cell Uptake Study	67
5.5.9. Anti-migration Test	68
6. RESULTS AND DISCUSSION	69
6.1. Particle Characterization	69
6.1.1. Lipid Selection	69
6.1.2. Drug Load Study	72
6.1.3. ALE decorated Nanoparticles	75
6.1.4. Encapsulation Efficiency	79
6.1.5. Differential Scanning Calorimetry (DSC)	80
6.1.6. Hydroxyapatite Affinity Study	82
6.1.7. Drug Releasing Study	84
6.1.8. Morphology	86
6.2. <i>In Vitro</i> Cell Study	88
6.2.1. Anti-cancer Efficacy Study	88
6.2.2. Toxicity Study	92
6.2.2.1. MTT Assay	92
6.2.2.2. Clonogenic Assay	94
6.2.3. Uptake Study	97

6.2.4. Anti-migration Test	99
6.3. Bone Binding Study	100
7. CONCLUSIONS	102
REFERENCE LIST	105

LIST OF TABLES

Table	Page
1-1. Summary of commonly used treatment for breast cancer	13
2-1. Physicochemical properties of TPL.....	20
2-2. Partition coefficients (Log P) of TPL between solid lipids and water.....	32
3-1. Summary of regularly used nano-carriers for PWSD delivery	38
3-2. Commercial available product of nanoemulsion formulation.....	41
5-1. HPLC method for Triptolide.....	61
5-2. Drug formulation used in clonogenic assay.....	67
6-1. Lipid selection study design	71
6-2. Formulation design for drug load study.....	73
6-3. Study designed for ALE decorating.....	76

LIST OF FIGURES

Figure	Page
1-1. Epidemiology information of cancer incident and death rate in 2017.....	2
1-2. 5 year % survival rates for different stage of breast cancer.....	3
1-3. Potential metastatic site for stage IV breast cancer.....	4
1-4. Different subtypes of breast cancer and aggressiveness.....	6
1-5. Process of metastatic breast cancer development.....	8
1-6. Bone microenvironment of normal condition and bone metastatic condition.....	10
1-7. Diagram of breast cancer radiation therapy.....	14
1-8. Doxil® doxorubicin HCl liposome injection.....	15
2-1. Triptolide information.....	19
2-2. Minnelide.....	20
2-3. Effect of TPL on proliferation and colony formation of tumor cells.....	24
2-4. Triptolide suppressed PC-3 tumor progression in mouse xenograft model.....	25
2-5. Effect of Triptolide on cells that express the MDR1.....	26
2-6. Determination of the effect in TPL combined with 5-FU on KB-7D cells <i>in vitro</i>	28
2-7. Triptolide inhibits osteoclastogenesis induced by tumor cells.....	29
2-8. Minnelide is synthesized from its parent compound.....	31
2-9. Mean Plasma Concentration–Time Profiles of Triptolide in Rats after Oral Administration of Triptolide.....	33
2-10. Mean Plasma Concentration–Time Profiles of Triptolide in Rats after <i>i.v.</i>	34
2-11. TPL application obstacles.....	35
2-12. The concentration of TPL in rat tissues following oral administration.....	36

3-1.	Schematic image of NLC with targeting decoration on the surface.....	40
3-2.	Product of Diprivan®.....	42
3-3.	Structure of Alendronate.....	43
3-4.	Illustrating image of bone matrix with HA and ALE binding route.....	43
3-5.	Amine crosslink reaction with NHS.....	45
3-6.	MTT reduction happened in mitochondria of the cells.....	49
5-1.	Bath sonicator. Branson 2800.....	54
5-2.	Example of microfluid chip design.....	56
5-3.	Alendronate conjugation amine crosslinking reaction with DSPE-PEG-NHS.....	57
5-4.	Zetasizer® 3000HS.....	59
5-5.	Centriprep® centrifugal filter.....	60
5-6.	Hitachi S4700 Scanning Electron Microscope with Gatan Alto 2500 cryo-system.....	63
5-7.	Filters with sample were fixed onto the sample platform, coated with gold platinum.....	64
5-8.	SpectraMax plate reader.....	65
6-1.	Structure of Docosahexaenoic acid (DHA).....	70
6-2.	DHA anti-cancer effect with BxPc3-RFP pancreatic cancer cell line.....	70
6-3.	Size stability study for lipid selection.....	72
6-4.	Size and encapsulation efficiency of different drug load formulation.....	74
6-5.	Size stability study for ALE decorating formulation.....	77
6-6.	Surface charge stability for ALE decorating formulation.....	78
6-7.	Encapsulation efficiency study for F5, 8, 9, 10.....	79
6-8.	DSC graph for blank particle and TPL-NP without ALE decoration.....	81
6-9.	Binding efficiency study.....	83
6-10.	Photo image of TPL-NP-ALE binding HA powder.....	83

6-11.	Drug releasing profile for different formulations.....	85
6-12.	Cryo-SEM images of TPL-NP.....	87
6-13.	MTT results with different cell lines.....	90
6-14.	MTT results for different formulations against MDA-MB-231 cell line.....	91
6-15.	MTT results for toxicity study against MC3T3 cell line.....	93
6-16.	Particle size differences between formulation tested in toxicity study.....	94
6-17.	Images of clonogenic assay results.....	95
6-18.	Colony number comparison between different treatment group.....	96
6-19.	Uptake comparison of MDA-MB-231 and MC3T3 cell lines.....	98
6-20.	Anti-migration test images.....	100
6-21.	Binding efficacy study with rats' leg bones.....	101
7-1.	Size distribution (intensity) of 8% ALE-NP-TPL.....	103



CHAPTER 1. BONE METASTATIC BREAST CANCER

1.1. Introduction

Breast cancer, among all cancer type, is the most common cancer and second most lethal type of cancer among women. As shown in [Fig 1-1.](#), almost one-third new incidents in 2017 are breast cancer in women [[Cancer Statistics, 2017](#)]. Although significant progress has been made over decades for treating the disease, 14 % women died diagnosed with breast cancer in 2017, ranking in second place.

Currently, efficient treatment has been developed for early stage breast cancer. As shown in [Fig 1-2.](#), for stage 0 and stage 1, when the tumor cells stay local and are not invading the wall of the tissue, 5-year survival rate can achieve as high as 100% [[Breast cancer, 2018](#)]. However, as the cancer develops and spreads, the survival rate goes down significantly. [Fig 1-3.](#) shows the potential metastatic site of breast cancer [[Breast Cancer Metastasis, 2016](#)]. In stage IV, which the cancer cell has metastasize to other vital organs, the survival rate dropped to only 22% after 5 years.

Estimated New Cases

		Males		Females			
Prostate	161,360	19%			Breast	252,710	30%
Lung & bronchus	116,990	14%			Lung & bronchus	105,510	12%
Colon & rectum	71,420	9%			Colon & rectum	64,010	8%
Urinary bladder	60,490	7%			Uterine corpus	61,380	7%
Melanoma of the skin	52,170	6%			Thyroid	42,470	5%
Kidney & renal pelvis	40,610	5%			Melanoma of the skin	34,940	4%
Non-Hodgkin lymphoma	40,080	5%			Non-Hodgkin lymphoma	32,160	4%
Leukemia	36,290	4%			Leukemia	25,840	3%
Oral cavity & pharynx	35,720	4%			Pancreas	25,700	3%
Liver & intrahepatic bile duct	29,200	3%			Kidney & renal pelvis	23,380	3%
All Sites	836,150	100%	All Sites	852,630	100%		

Estimated Deaths



		Males		Females			
Lung & bronchus	84,590	27%			Lung & bronchus	71,280	25%
Colon & rectum	27,150	9%			Breast	40,610	14%
Prostate	26,730	8%			Colon & rectum	23,110	8%
Pancreas	22,300	7%			Pancreas	20,790	7%
Liver & intrahepatic bile duct	19,610	6%			Ovary	14,080	5%
Leukemia	14,300	4%			Uterine corpus	10,920	4%
Esophagus	12,720	4%			Leukemia	10,200	4%
Urinary bladder	12,240	4%			Liver & intrahepatic bile duct	9,310	3%
Non-Hodgkin lymphoma	11,450	4%			Non-Hodgkin lymphoma	8,690	3%
Brain & other nervous system	9,620	3%			Brain & other nervous system	7,080	3%
All Sites	318,420	100%	All Sites	282,500	100%		

Fig 1-1. Epidemiology information of cancer incident and death rate in 2017.

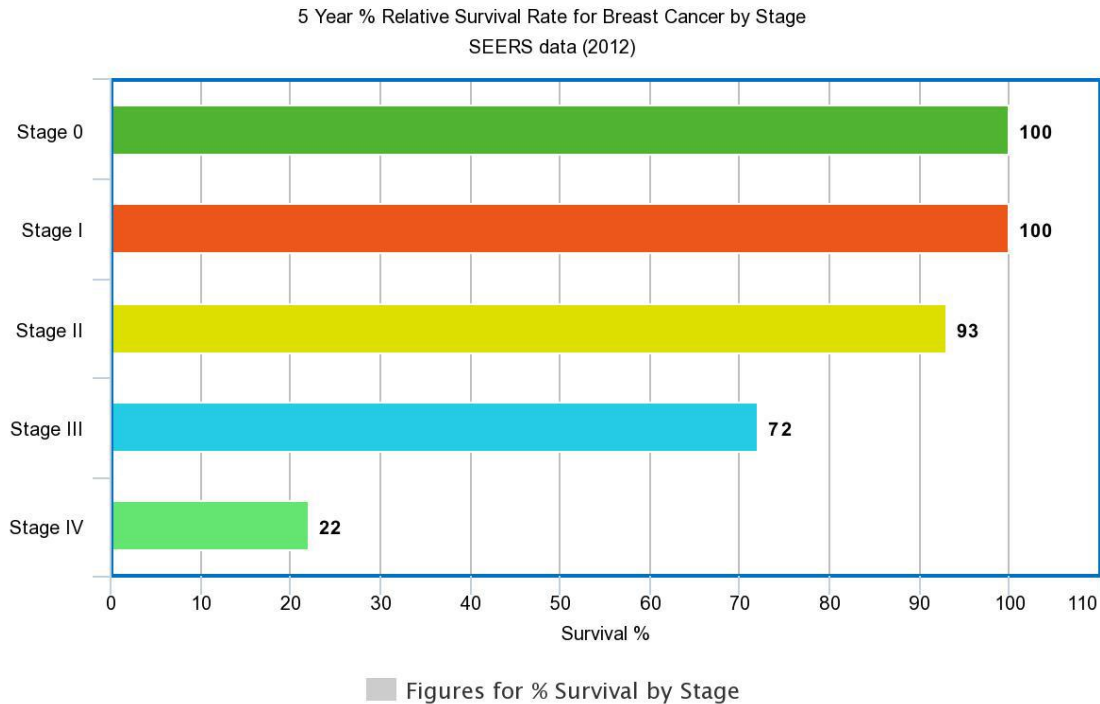
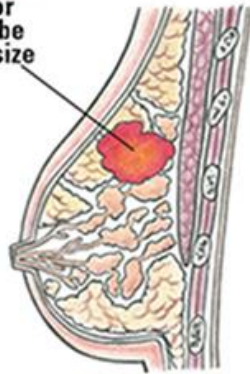


Fig 1-2. 5 year % survival rates for different stage of breast cancer.

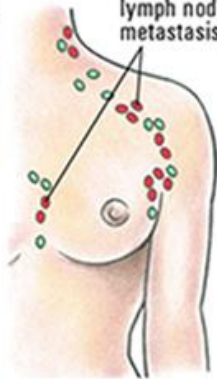
In late stage II and stage III, cancer cells invade the regional wall and blood veins to get access to the blood circulation. On the other hand, as lymphatic system is also located in the breast tissues abundantly, evidence has shown that tumor cells can also metastasize through lymphatic system. In general, the most common metastatic locations are brain, lung, liver and bones.

STAGE IV METASTATIC BREAST CANCER

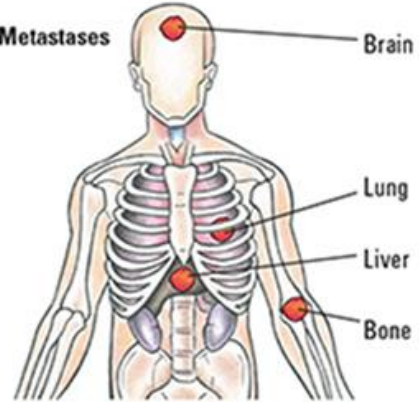
Stage IV
Tumor
may be
any size



Possible
multiple
lymph node
metastasis



Metastases



©Patient Resource LLC

Fig 1-3. Potential metastatic site for stage IV breast cancer.

1.2. Mechanism and Rational

1.2.1. Metastatic Breast Cancer

1.2.1.1. Various types of breast cancer

Breast cancer can be divided into different subtypes based on distinct gene expression profiles. [Figure 1-4](#) shows the classification of different types of breast cancer [[Dai, Xiaofeng, 2017](#)].

The least aggressive type is the estrogen receptor (ER) -positive breast cancer. Among the ER-positive tumors, it can be divided into two types, luminal A and B. A type has higher ER expression and low expression of proliferative genes. Cancer cells use the hormone estrogen to proliferate and grow in this type, making those hormone receptors a potential target for the treatment. For ER negative cells, they tends to have higher progesterone receptor (PR) and human epidermal growth factor 2 (HER-2) expression. Although the estrogen-based treatment will show no response, the cancer cells are highly hormone dependent on other growth factors. At the early stage while the cancer cells are ER, PR or HER-2 positive, the treatment of the breast cancer is usually hormone receptor blocker that inhibit the binding of those hormones and then inhibit the growth.

Once all three receptors' expressions are down-regulated, it was classified into triple negative breast cancer, which is known to be the most difficult type to treat. Since a large number of current treatments target hormone or growth factor receptor mentioned

above, it is essential to determine what subtype of the tumor before applying the suitable treatment. For the triple negative breast cancer, regular chemo-drug is usually used since the hormone targeted therapy will not have any responses. For most late stage breast cancer, triple negative subtype has become an obstacle for increasing the survival rate.

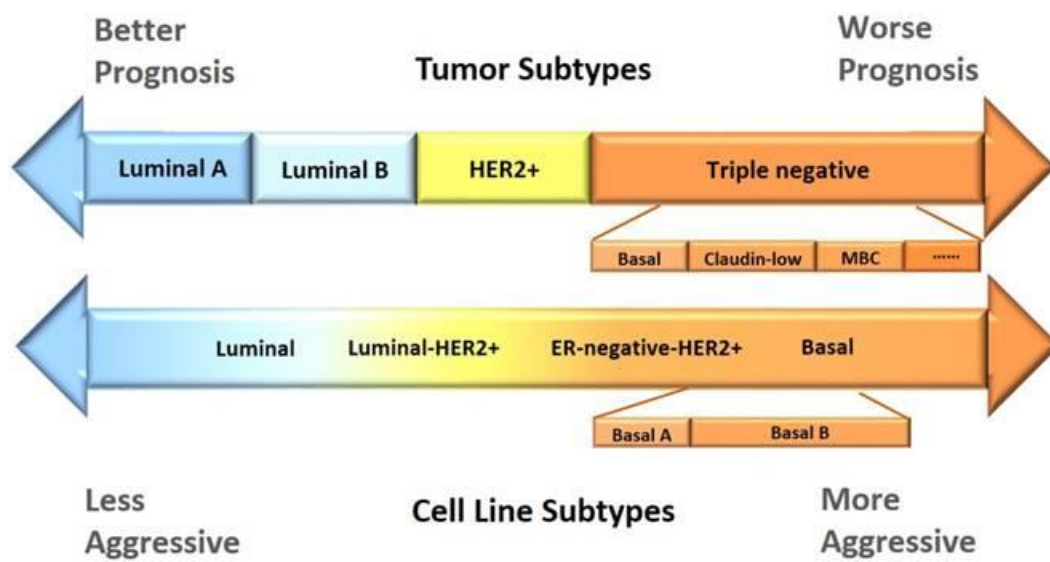


Fig 1-4. Different subtypes of breast cancer and aggressiveness.

1.2.1.2. Mechanism of metastatic breast cancer (MBC)

Metastasis of tumor usually comprised of a series of sequential steps. [Fig 1-5](#) shows the process of MBC development [[Scully O J, 2012](#)]. Tumor cells initially start in the epithelial cell of the milk duct at the early stage. At ductal carcinoma in situ (DCIS) stage, the tumor cells are not invasive. Metastasis starts with the local invasion from the primary tumor to the surrounding blood or lymphatic vessels. As tumor development usually involves angiogenesis around the tumor area, cancer cells can invade the blood vein surrounding the tumor area. Cancer cells will then circulate around the body and relocated to the other organs by extravasating in to the organ parenchyma. At metastatic site, the invasive tumor cells will form niche at local microenvironment and then developing into new local tumor. Since the secondary tumors are formed from invasive cancer cells, the metastatic cancer cells are usually highly aggressive and resistant to therapy.

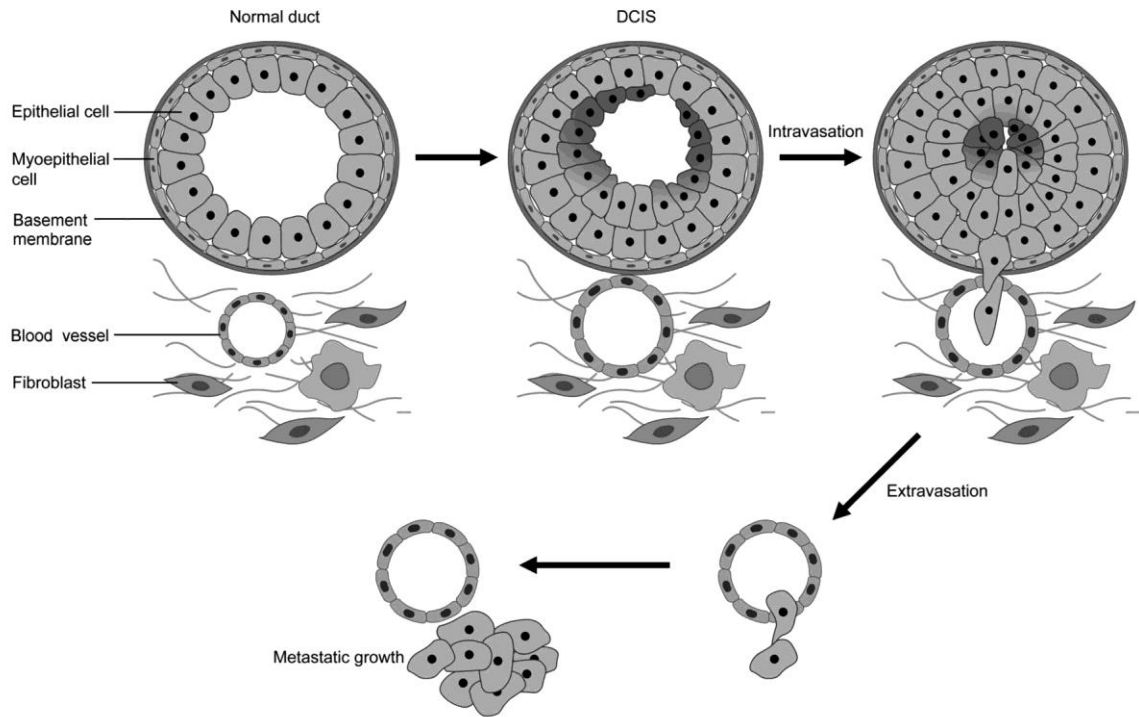


Fig 1-5. Process of MBC development.

1.2.1.3. Bone Metastasis

Bone metastasis is the most frequent site of breast cancer metastasis [Parkes, Amanda, 2018]. In one study it was found that 60-80% patients with MBC are having bone metastasis [Manders, Klaartje, 2006]. In another study, 51 % of the patients with bone relapse after the treatment of breast cancer were found to be bone only metastasis (BOM) [Coleman R E, 1987]. Bone MBC constituted the single largest risk factor for increased morbidity and mortality. As reported before, several factors account for the

high frequency of bone metastasis [Roodman G D., 2004]. Blood flow in the area of bone marrow is high, creating high probability of metastasis. On the other hand, the extracellular matrix excreted by tumor cells increase the adhesiveness to the marrow stromal cells and bone matrix. This interaction further increases the angiogenic factors and bone-resorbing factors produced by tumor cells, thus resulting in bone metastasis enhancement. Moreover, bone microenvironment is rich with growth factors such as transforming growth factor β , insulin-like growth factors I and II, *etc.* that favor the proliferation of cancer cells.

Generally speaking, tumor metastasis leading to bone loss are classified as osteolytic while in contrast those leading to excess bone deposition are osteoblastic. The mechanism and consequences of the bone MBC was extensively studied. The majority of the bone MBC was classified as osteolytic, which caused bone loss ultimately. Fig 1-6. summarizes the mechanism of bone BMC causing bone loss in the microenvironment and one of the treatments [Chen, Yu-Chi, 2010]. Under normal condition, the differentiation and function between osteoclast and osteoblast are in a balance, which will maintain the structure of the bone matrix.

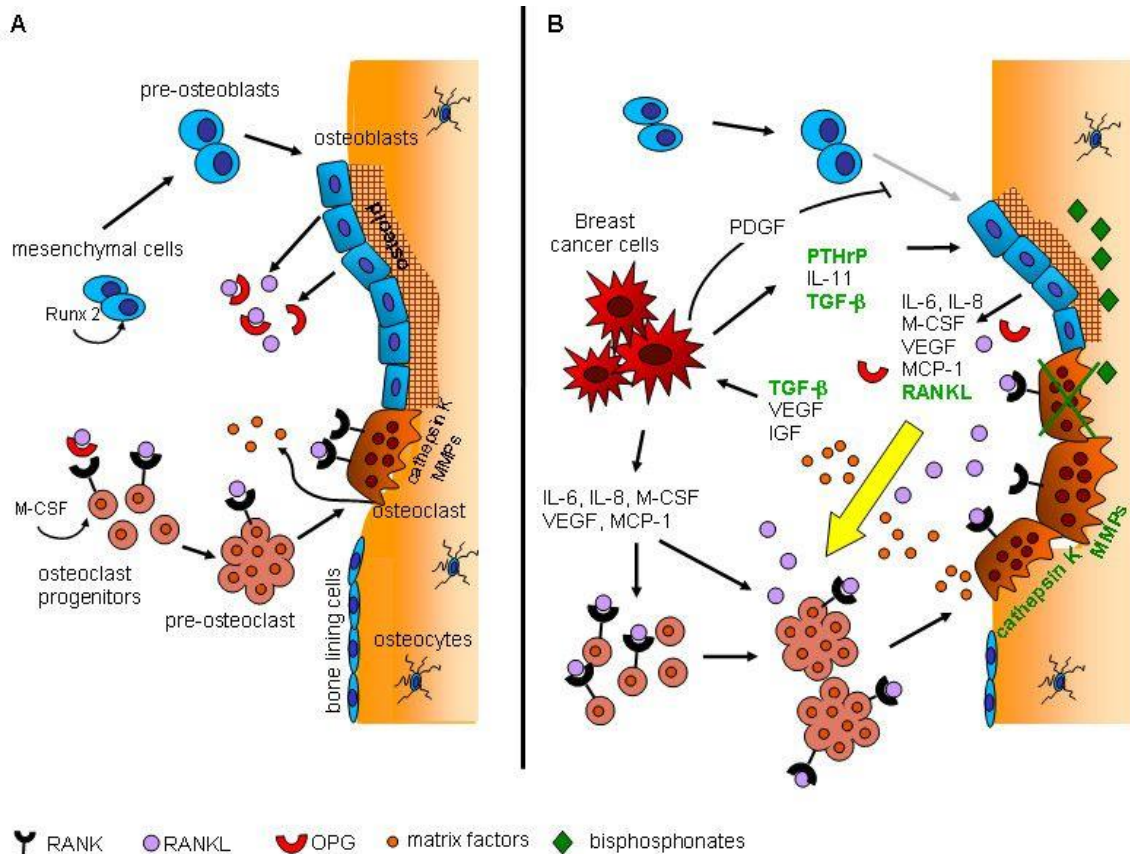


Fig 1-6. Bone microenvironment of normal condition and bone metastatic condition.

A) The bone microenvironment under conditions of normal bone remodeling; B) Bone microenvironment in the presence of osteolytic bone metastases. RANKL: Receptor activator of nuclear factor kappa-B ligand; TGF: Transforming Growth factor; M-CSF: Macrophage Colony-Stimulating Factor; MCP1: Monocyte chemoattractant protein 1, cytokine also known as CCL2; IL: interleukin; IGF: Insulin-like growth factor; PTHrP: Parathyroid hormone-related protein.

However, with the presence of the breast cancer cells in the microenvironment, the balance was broken because of the overexpression of some growth factors from the tumor cells. The ratio between osteoprotegerin (OPG) and RANKL determines the activity of osteoclast and osteoblast. OPG is a decoy receptor to RANKL. As shown in the figure, breast cancer cells secrete PTHrP, cytokines and other growth factors that negatively impact osteoblast function. On the other hand, ligand such as RANKL and other pro-osteoclastogenic cytokines were increased and stimulate the differentiation of the osteoclast. Thus, the bone loss in osteolytic metastasis breast cancer is mediated and caused by the osteoclasts rather than tumor cells.

1.2.2. Current treatment and obstacles

As summarized in [Table 1-1](#), current treatments for breast cancer involve in hormone-therapy (including ER, PR or HER2 receptor targeting), chemotherapy and other treatment such as radiation, surgery etc. However, each treatment has its limitations.

Radiation therapy focuses the radiation onto the tumor by achieving higher local intensity. The therapy can kill a large proportion of cancer cells within the tumor area. However, the therapy inevitably damages surrounding areas. The application of therapy also faces great limitation when the cancer cells are spreading and metastasizing to areas such as the brain.

Table 1-1. Summary of commonly used treatment for breast cancer.

Treatment	Drugs	Mechanisms	Side Effect	Disadvantage
Hormone-therapy	Tamoxifen, Leuprolide	Block hormone receptor and inhibit the proliferation of cancer cells	Menopausal symptom, hot flashes...	Only effective to ER-positive or PR-positive cancer
Anti-HER2	Trastuzumab Pertuzumab	Attached to the HER2 protein, slows or stops the growth of cancer cells	Less than chemotherapy	Only effective to HER2-positive cancer
Chemotherapy	Doxil, Paclitaxel, 5FU	Various pathway, apoptosis or anti-proliferation	Drug-dependent	Resistance, systemic toxicity
Others	Radiation	Damage the DNA or genes that are responsible for the replication or growth of cells	Acute, long-term, accumulate side effect	Radiation-induced cancer

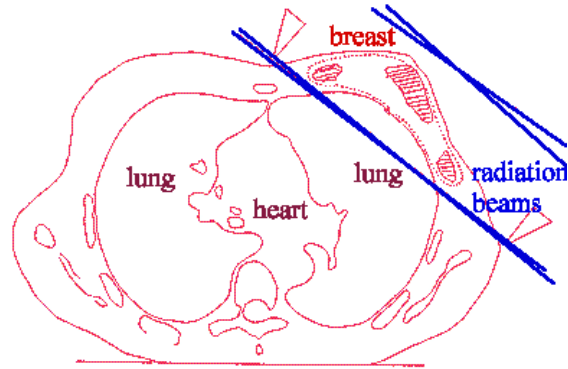


Fig. 1-7. Diagram of breast cancer radiation therapy [\[About cancer\]](#).

Surgery is another first line of treatment for many solid tumors. Surgery can remove large volume of tumor that significantly reduce the symptom. However, the surgery is unable to kill microscopic tumor around the edges of solid tumors or metastatic cells. In addition, the surgery may involve in removal of part of whole piece of organ that may affect the life quality of the patient post-surgery.

Hormone receptor targeting drug (example listed in [Table 1-1](#)), it shows great anti-cancer effect by killing large number of cancer cells throughout the body. As the treatments are usually systemically delivered, the active ingredients can circulate around the body, reaching every location that the cancer exist. The limitation of the treatment, however, is also significant. It only works with the receptor positive cancer cells. As cancer develops, tumor cells can gain resistance by downregulating the receptor expression.

On the other hand, systemic chemotherapy can effectively kill cancer cells via various pathways. It usually involves apoptosis or anti-proliferation. However, side effects caused by the chemo compound have limited the application of these drugs. It can cause systemic toxicities to the patient during the treatment. Systemic treatment, including hormone therapies, may not kill all the tumor cells in the body, potentially leaving the opportunities for the cancer relapse after the treatment. In addition, cancer cell can gain resistance against some commonly used chemo-drugs such as Doxil®. The systemic treatments such as chemotherapy, hormone therapy or target therapy are usually combined with surgery and radiation therapy to further kill cancer cells in the body.



Fig. 1-8. Doxil® doxorubicin HCl liposome injection.

For bone MBC, bisphosphonates such as zoledronic acid (Zoledronate™) was used to relieve the symptom of osteoclastogenesis caused by breast cancer cells. It can bind to hydroxyapatite of bone matrix and digested by osteoclasts, leading to apoptosis. However, the treatment can only slow down the progression of osteolytic lesion and relieving the symptom but cannot bring healing to the patient. Thus, a better therapeutic method needs to be developed for more efficient anti-MBC treatment.

CHAPTER 2. TRIPTOLIDE

2.1 Introduction

Triptolide (TPL), a diterpenoid triepoxide that is extracted from a traditional Chinese herb called ‘Thunder God Vine’ (also known as *Tripterygium Wilfordii*) has recently drawn increasing interest from pharmaceutical and biomedical researchers, structure shown in Fig 2-1. [Liu, Zi, 2011]. Previous studies have reported efficacy of TPL for immunosuppressive, anti-inflammatory, and anti-fertility therapies [Li, Di-Cai, 2009]. In addition, promising anti-cancer effects of TPL have been demonstrated in *in vitro*, *in vivo* and pre-clinical studies [Zhou Z L, 2012]. TPL has shown significant tumor growth inhibition and anti-proliferative activities in a broad range of cancer cell types including melanoma, breast cancer, bladder cancer, gastric carcinoma, ovarian cancer, pancreatic cancer, multiple myeloma, acute and chronic myelogenous leukemia, glioblastoma multiforme, colon cancer, prostate cancer and metastatic lung and spleen cancer [Westfall, Suzanne D, 2007] [Phillips, Phoebe A., 2007] [YinJun, Lou, 2005] [Carter, Bing Z, 2008] [Shi, Xianping, 2009] [Lin, J., 2007] [Wang, Zhipeng, 2009] [Huang, Weiwei, 2012]. Early clinical studies in the USA and China also reported growth inhibition of solid tumors in TPL-treated subjects [Lu, L. H., 1992].

Recently, researchers have been investigating the osteoclasto-genesis effect of triptolide for its potential bone defect treatment. Evidences have shown that TPL can

regulated the osteoclast differentiation pathway and therefore inhibit the osteoclastogenesis effect induced by tumor cells in the bone microenvironment [Park B, 2014]. This new mechanism can potentially expand the application of triptolide to bone cancer treatment and locally delivery/injection formulation.

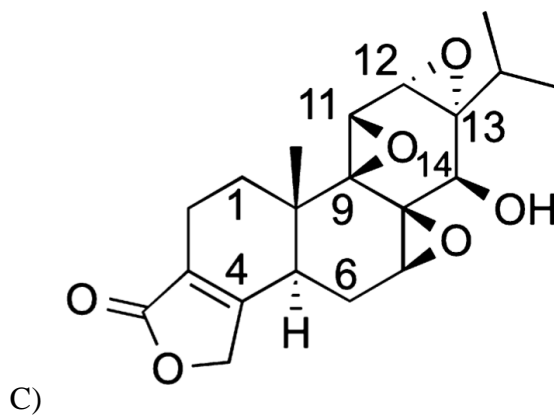


Fig 2-1. Triptolide information. A) *Tripterygium Wilfordii* Hook F: Thunder God Vine

B) Chinese medicine of Thunder God Vine. C) Chemical structure of triptolide.

Table 2-1. Physicochemical properties of TPL.

Triptolide Physicochemical Properties	
Molecular Weight	360.41
Solubility	17 µg/mL
LogP	0.6
Melting Point	227 °C

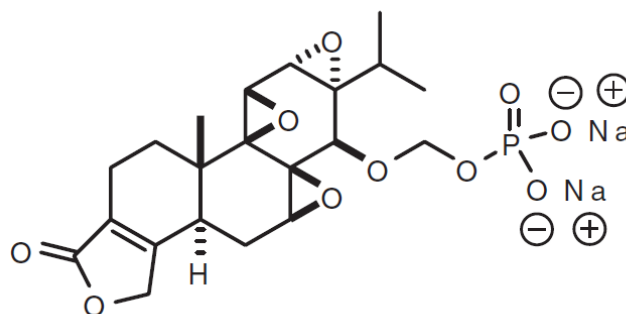


Fig 2-2. Minnelide: 14-*O*-phosphonoxymethyltriptolide disodium salt [Chugh, Rohit, 2012].

Although TPL has shown outstanding efficacy for killing cancer cells, its poor aqueous solubility (0.017 mg/mL aqueous), non-specific biodistribution and the associated toxicity have limited its therapeutic application. To overcome these issues, two

different directions have been explored. On one hand, scientists are trying to develop prodrugs for TPL (example shown in Fig 2-2.) [Chugh, Rohit, 2012]. While this may improve the drug solubility, the biodistribution and toxicity issues of the compound may persist. On the other hand, nano-delivery system is considered to be utilized to target deliver TPL. Lipid-based nanocarriers such as nanostructured lipid carriers have been extensively studied for delivery of poorly-water soluble drug compounds [Narvekar, Mayuri, 2014]. The delivery system was often made with a combination of physiological lipids, phospholipids and/or oils thus they are highly biocompatible and biodegradable with minimal toxicity and immunogenicity problems. This class of nano-delivery systems can also be easily surface-modified for extended circulation and targeted delivery to enhance the cancer specificity.

2.2 Anti-cancer effect

Triptolide has been proved as an efficient chemo-agent for various type of cancer cell lines. Multiple studies have been reported regarding the mechanism of anti-cancer effect of Triptolide:

1. Anti-proliferation effect of cancer cells leading to apoptosis;
2. Insensitiveness to Multi-Drug Resistance (MDR1) gene, low resistance;
3. Sensitizer effect with other traditional chemo-drugs.

Anti-proliferation effect of cancer cells

Multiple researches have shown that TPL has potent cytotoxicity against a broad spectrum of tumor. In 2003, Yang and their group have discovered that TPL can inhibit DNA synthesis and colony formation of different melanoma cell line [Yang S, 2003]. As shown in Fig 2-3., the study was using 3H-thymidine incorporation assay to evaluate the proliferation of cancer cells. In A, MDA-435 tumor cells were treated for 2 days. The proliferation of the tumor cells was inhibited by TPL in a dose dependent manner. TPL has achieved much better anti-proliferation effect at 25 ng/mL than Taxol at 100 ng/mL. Similar results were obtained with B16F10 cells. In B, clonogenic assay was used to further evaluate the growth inhibition effect of TPL. B16F10 tumor cells were suspended in 0.36% agarose containing Taxol or TPL at the indicated concentrations for two weeks. Similar result has been observed that colony number of 2 ng/mL TPL group is only half of the 100 ng/mL Taxol treatment, suggesting even stronger anti-cancer effect. The high

potency of TPL can lower the dose of the treatment and achieve high chemo-treatment efficiency. However, this may also cause toxicity issues.

On the other hand, multiple studies have reported that TPL has anti-cancer effect against broad spectrum of cancer type. In 2012, Huang and their group have found that TPL can inhibit the proliferation of prostate cancer cells [Huang, Weiwei, 2012]. As shown in Fig 2-4., TPL showed significant tumor inhibition in mouse xenograft with PC-3 cells. Similar result has been reported with pancreatic cancer, ovarian cancer, multiple myeloma cancer, glioblastoma multiforme cancer, colon cancer, leukemia and breast cancer [Westfall, Suzanne D, 2007] [Phillips, Phoebe A., 2007] [YinJun, Lou, 2005] [Carter, Bing Z, 2008] [Shi, Xianping, 2009] [Lin, J., 2007] [Wang, Zhipeng, 2009] [Huang, Weiwei, 2012].

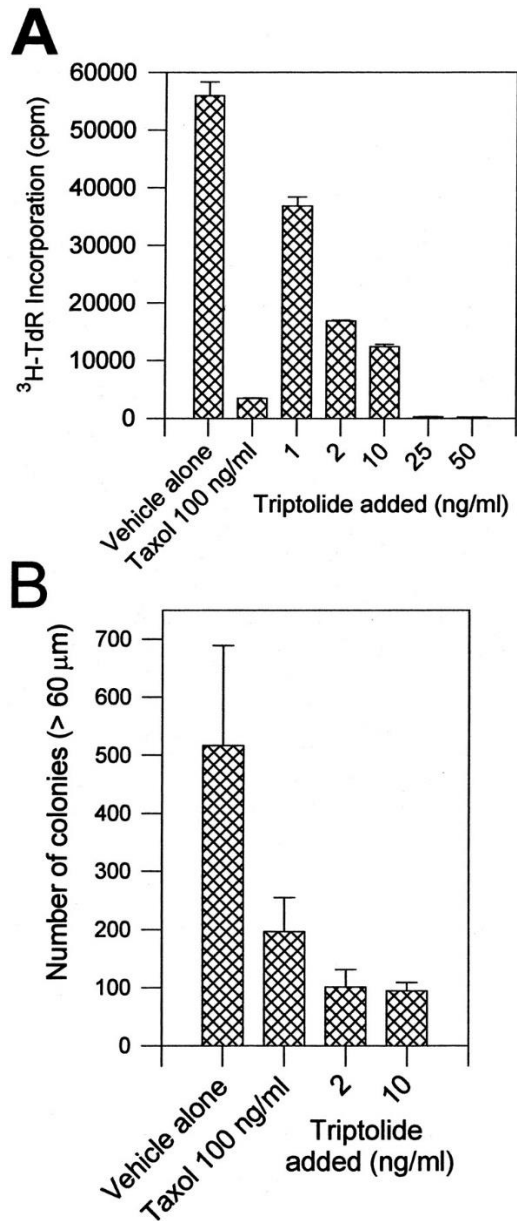


Fig 2-3. Effect of TPL on proliferation and colony formation of tumor cells. All of the experiments were repeated three times. Similar results were obtained in other tumor cell lines, such as 4T1 and TSU cells [Yang S, 2003].

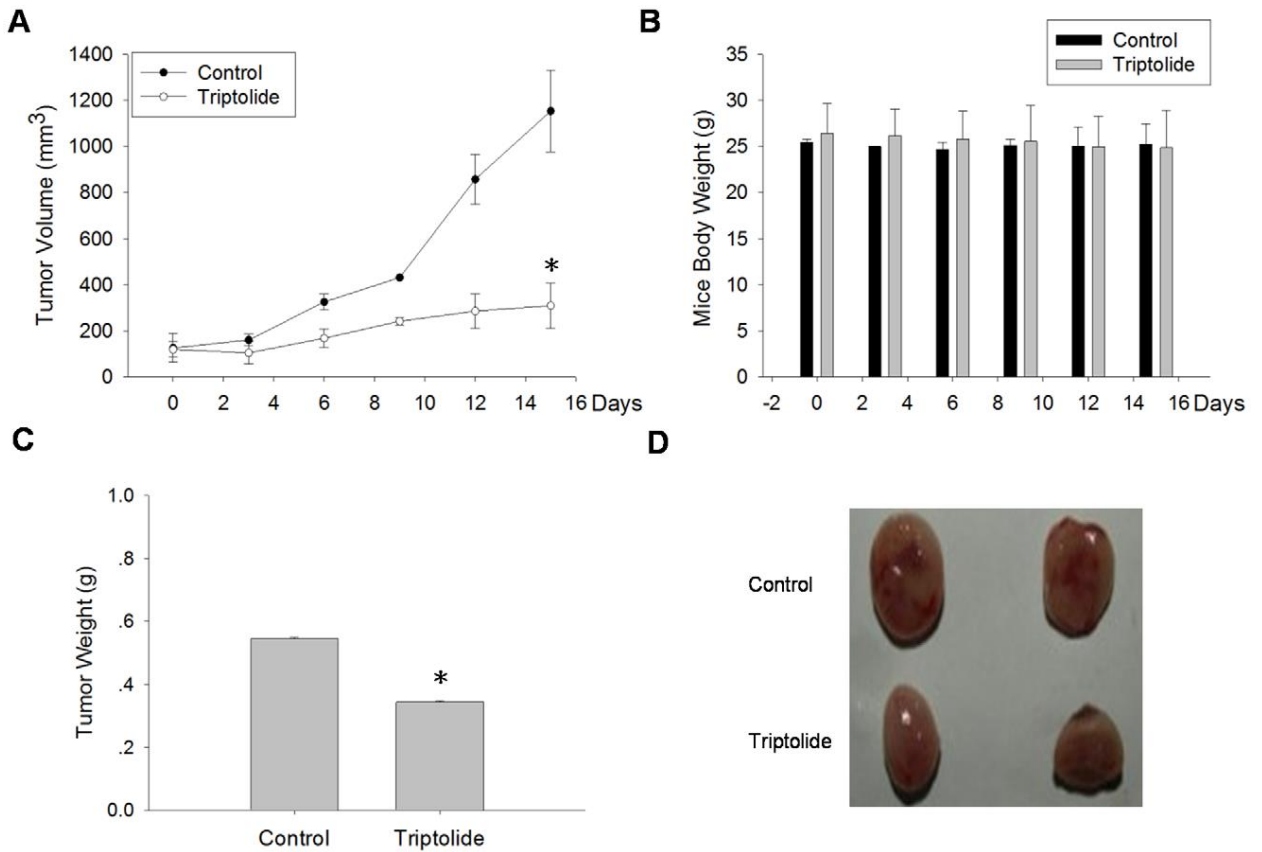


Fig 2-4. Triptolide suppressed PC-3 tumor progression in mouse xenograft model. PC-3 cells (2×10^6 per mouse) were injected into 5-week-old nude mice. When solid tumors grew to about 100 mm³, the mice were treated intraperitoneally with either a vehicle control or Triptolide at 0.4 mg/kg daily for 15 days. Tumor sizes and body weight were measured every three days. (A) Effect of Triptolide on xenograft tumor volume. (B) Effect of Triptolide on nude mice body weight. (C) Effect of Triptolide on xenograft tumor weight. (D) Image of xenograft tumor treated with or without Triptolide.

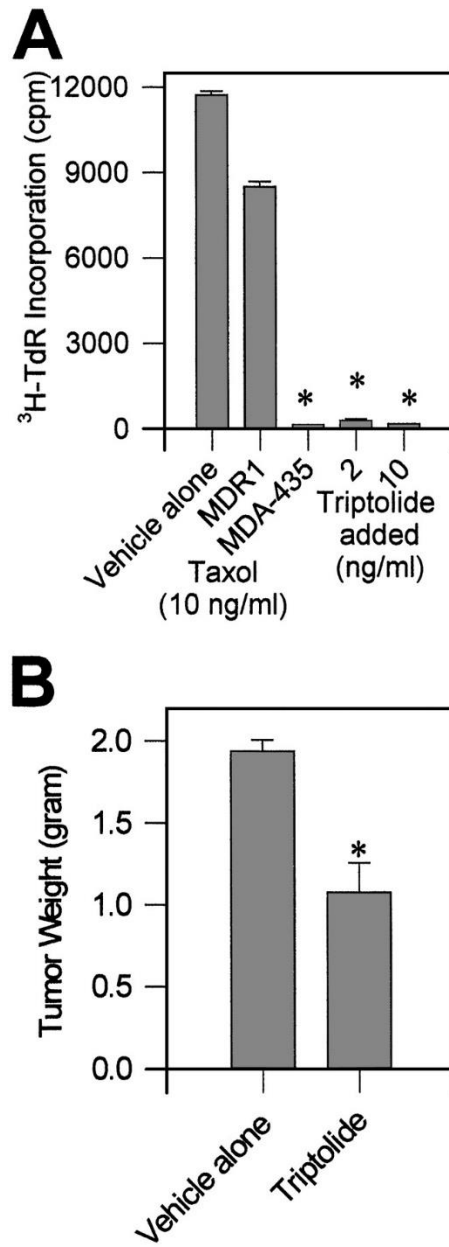


Fig 2-5. Effect of TPL on cells that express the MDR1. A pair of MDA-435 cells that had been transfected with either a control retrovirus vector or one containing the MDR1 were tested for their sensitivities to TPL.

Insensitiveness to Multi-Drug Resistance (MDR1) gene

For regular chemo-therapy drug, MDR1 gene plays a significant role in drug resistance occurrence. For instance, paclitaxel and docetaxel, which are the most commonly used chemo-drug, resistances have been reported, mainly mediated by the expression of the MDR phenotype [Galletti, Elena, 2007]. In contrast, TPL has been reported to downregulate the expression of MDR1 gene in prostate cancer cells, making it insensitive to chemo-resistant tumor cells [Guo, Qingpeng, 2013]. In another paper, TPL showed much more efficient proliferation inhibition effect at the same concentration, shown in Fig 2-5. [Yang S, 2003]. Regular chemo-compound taxol showed limited anti-cancer effect with MDR1 transfected MDA-435 cells, while TPL remained highly potent anti-cancer effect. The insensitiveness of TPL can help prevent the common resistance of cancer cells.

Sensitizer effect with other traditional chemo-drugs

In addition of insensitiveness of TPL to MDR1, TPL can also serve as a chemo-drug sensitizer and used as a combination therapy by inhibiting the MDR1 gene expression and downregulating the P-gp transporters. In 2010, Chen and their group discovered that TPL can enhance 5-fluorouracil (5-FU) antitumor effect with KB cells. As shown in Fig 2-6., with the low concentration treatment of TPL, 5-FU showed double anti-tumor effect *in vivo* with mice [Chen Y W, 2010].

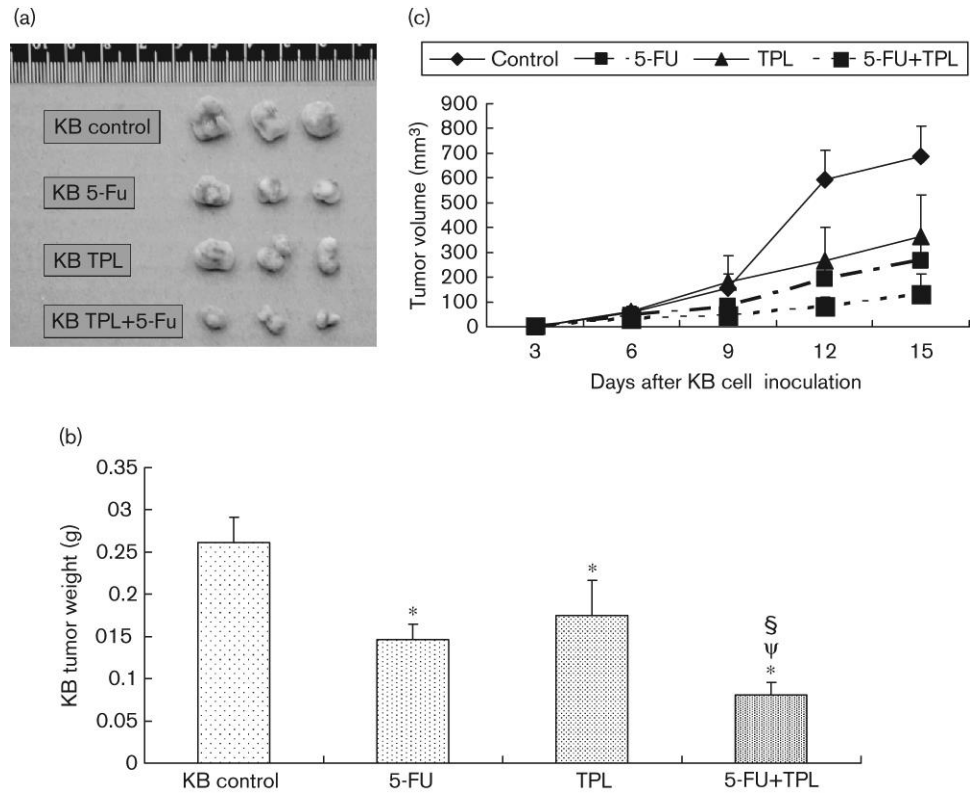


Fig 2-6. Determination of the effect in TPL combined with 5-FU on KB-7D cells in vivo.

(a) KB-7D xenograft-bearing NOD/SCID mice were treated daily with TPL (0.075 mg/kg), 5-FU alone (12 mg/kg) or combination of both as well as solvent control, and the tumors were examined on day 15. (b) The average of tumor weight shown in (a) was compared between TPL, 5-FU treated alone or combination (c) Tumor volume of KB-7D xenograft treated in vivo with TPL and 5-FU or not [Chen Y W, 2010].

2.3 Osteoclast inhibition

Recently, researchers have found that TPL can inhibit the osteoclastogenesis induced by breast cancer cells migrated to bone microenvironment [Park B, 2014]. As discussed before, metastasized breast cancer cells can secrete VEGF and other growth factor, inducing the differentiation of osteoclast progenitors into osteoclast. This will break the balance between osteoclast and osteoblast. In 2014, Byoungduck Park reported that TPL can inhibit osteoclastogenesis by inducing RANKL (Receptor activator of nuclear factor – kappa B ligand) signaling. RANK-RANKL signaling can activated a variety of downstream signaling pathways required for osteoclast development.

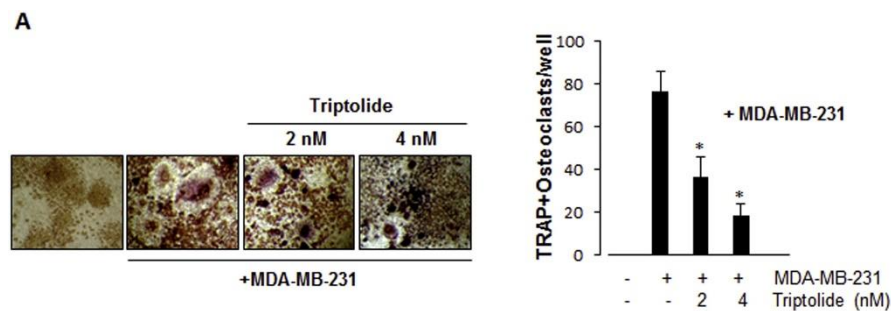


Fig 2-7. Triptolide inhibits osteoclastogenesis induced by tumor cells. RAW 264.7 cells (5×10^3) were incubated in the presence of breast cancer (MDA-MB-231) cells (1×10^3 ; upper) for 24 h, then exposed to triptolide (2, 4 nmol/L) for 5 days, and finally stained for TRAP expression. Multinucleated osteoclasts (i.e., those containing three nuclei) in cocultures were counted [Park B, 2014].

As shown in [Fig 2-7.](#), MDA-MB-231 (aggressive breast cancer cell line) can induce the differentiation of osteoclast (multinucleus before the treatment. However, with low concentration treatment of TPL, the count of osteoclast (multinucleated cells) decrease as the concentration increase. This make it possible to use TPL for breast cancer bone metastasis since it can not only inhibit tumor cell proliferation, but can also relieve the symptom of bone osteoclast caused by breast cancer.

2.4 Current obstacle of TPL

Solubility issue in water

In spite of the outstanding antitumor effect of TPL, major obstacles exist preventing the application of the drug. The solubility of the drug is relatively low, reported as 0.017 mg/mL. This may cause challenges for formulation design of the API. In order to overcome the solubility problem, a pre-drug has been developed, as shown in Fig 2-8. Although the prodrug can enhance the solubility of the API, it may not solve other problem of TPL

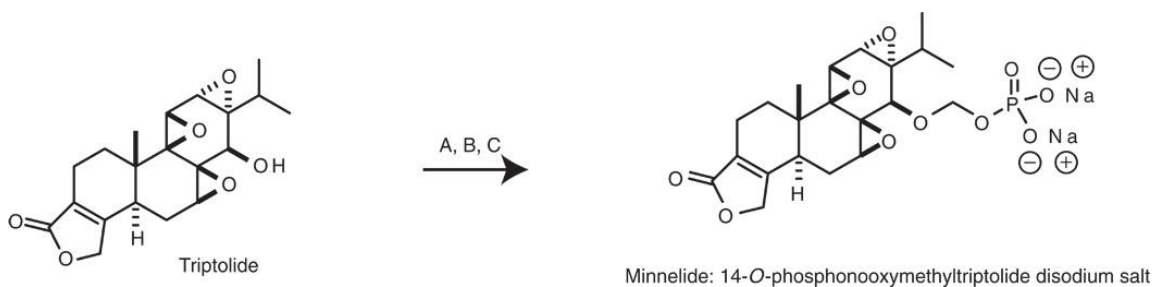


Fig 2-8. Minnelide is synthesized from its parent compound, triptolide. Schematic of the synthesis of Minnelide from triptolide. (A) DMSO, Ac₂O, AcOH, 5 days, 52%. (B) Dibenzylphosphate, 4-Å molecular sieves, N-iodosuccinimide, dichloromethane, tetrahydrofuran, 5 hours, 80%. (C) (i) H₂, Pd/C, room temperature, 3 hours; (ii) NaCO₃, 90%; purity of Minnelide >95% (by HPLC). [Chugh, Rohit, 2012].

Solubility issue in oil

In order to develop a nanoparticle delivery system that can encapsulate the API efficiently, the compound needs to dissolve in the oil core matrix well. However, TPL has been reported to have poor oil/water partition coefficient with most common used oil excipient, shown in [Table 2-2 \[Zhang C, 2014\]](#). This can result in low drug loading and low encapsulation efficiency of the particle system. In order to solve the problem, a lipid needs to be selected for better dissolving the API.

Table 2-2. Partition coefficients (Log P) of TPL between solid lipids and water.

Solid lipids	Palmitric acid	Compritol 888 ATO	Precirol ATO 5	Stearic Acid
Log P	0.66 ± 0.03	0.80 ± 0.05	0.67 ± 0.04	0.63 ± 0.01

Rapid absorption and elimination

In 2007, Feng Shao and their group reported the pharmacokinetic study of TPL in rats [[Shao F, 2007](#)]. Two administration routes have been tested, namely intravenously and orally. For oral delivery, the half-life of absorption was reported as 2-3 min while the

elimination half-life was 16-20 min in rats (shown in Fig. 2-9). On the other hand, the half-life for *i.v.* dose was around 15.1 min (shown in Fig. 2-10). The bioavailability was reported as 72.08% for 0.6 mg/kg dose. The significant short half-life of the drug may cause challenges in application of the compound. Although the bioavailability is relatively high, half-life for TPL remains relatively short. What's more, TPL might be toxic to the GI tract during absorption. Thus, a new formulation using other administration route needs to be developed.

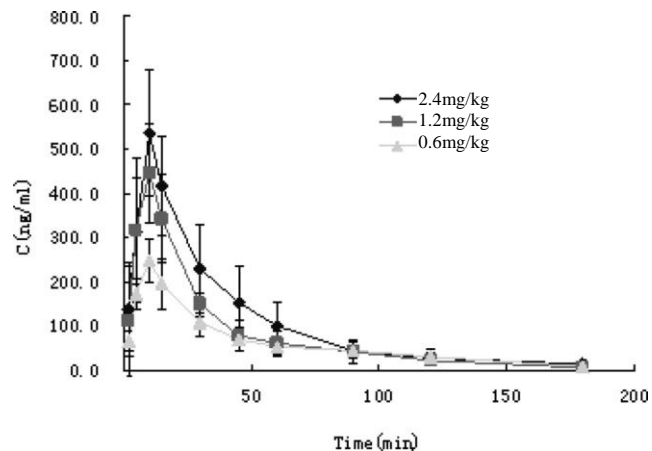


Fig 2-9. Mean Plasma Concentration–Time Profiles of Triptolide in Rats after Oral Administration of Triptolide at Doses of 0.6 mg/kg, 1.2 mg/kg and 2.4 mg/kg, Respectively.

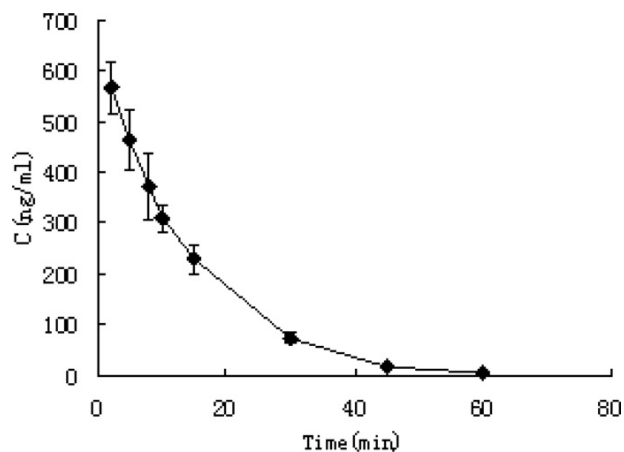


Fig 2-10. Mean Plasma Concentration–Time Profiles of Triptolide in Rats after i.v. Administration of Triptolide at Dosage of 0.6 mg/kg

Non-specific biodistribution and toxicity

On the other hand, TPL was also found to distribute into all vital organs, especially in liver and spleen [Shao F, 2007]. As shown in Fig. 2-12, although TPL has shown significant toxicity in all organs, the mechanism is still unclear. What's more significant, the toxicity produced by the TPL was lag behind the exposure concentration. It is well known that TPL has small margin between the therapeutic and toxic doses. Generally speaking, therapeutic index less than 3 is a reasonable cutoff to define narrow therapeutic index drugs. As mentioned in a review book, TPL was considered as a narrow therapeutic index (NTI) drug [Chi-hin, Cho, 2017]. With toxicity, short half-life and

narrow therapeutic index, TPL was difficult to formulate and be applied to anti-cancer treatment. In order to utilize the high efficiency of TPL in treating cancer cells, bone targeting nanoparticle with local injection was studied to optimize the API.

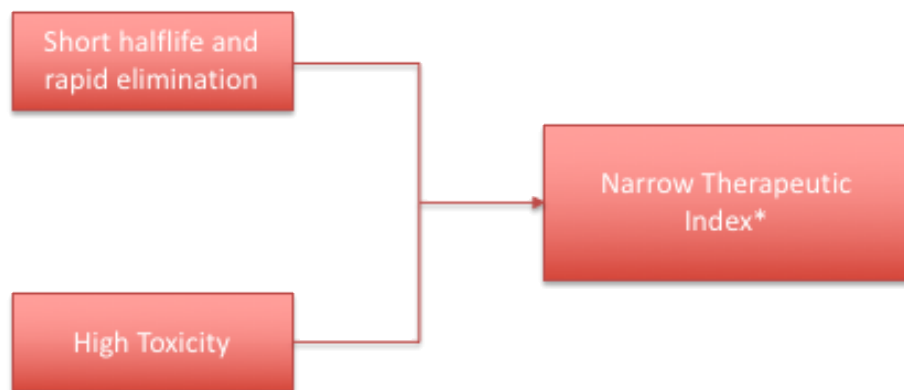


Fig. 2-11. TPL application obstacles.

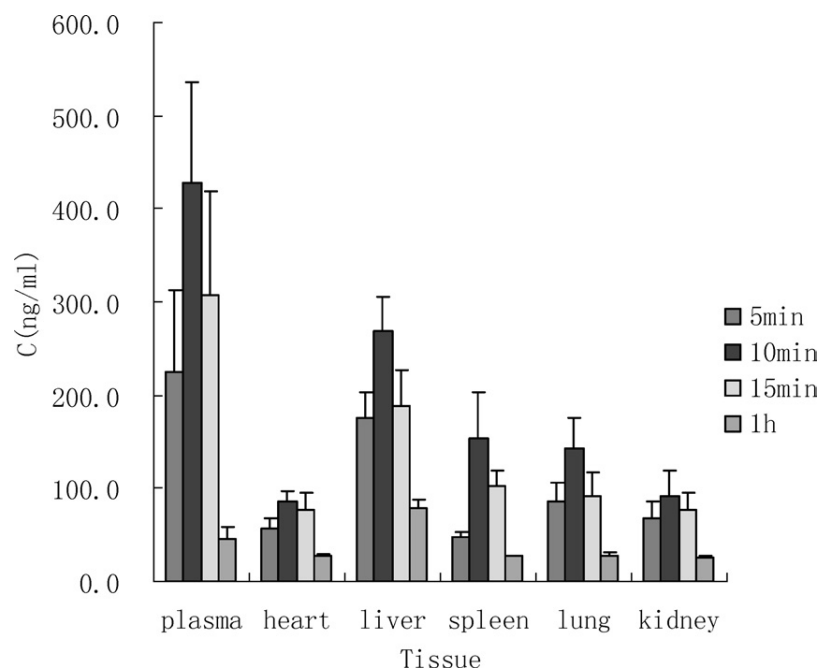


Fig. 2-12. The concentration of TPL in rat tissues following oral administration at the dose of 1.2 mg/kg (n=6, Mean \pm S.D.) [Shao F, 2007].

CHAPTER 3. BONE TARGETING NANOPARTICLE

3.1 Nano-structure lipid carrier

3.1.1 Introduction

In order to overcome the obstacle of TPL application, nano-structure delivery systems can be used to not only enhance the solubility of the API but can also actively targeting the tumor site in the bone micro environment. What's more, the nano-carrier can sustain release the API without repeat injection. This can effectively deliver the short half-life API such as TPL.

Table 3-1. Summary of regularly used nano-carriers for PWSD delivery.

Type	Charateristics	Drug delivered
Liposomes	Amphiphilic, biocompatible, Easy modification, Targeting potential Improve solubility Stability	Paclitaxel, ATRA Docetaxel, Etoposide Camptothecin Curcumin
Solid-lipid nanoparticles (SLN)	Easy scale-up High lipid content, good encapsulation Nontoxic organic solvent	Paclitaxel, Docetaxel Curcumin Camptothecin
Nanostructured lipid carrier	Higher drug loading than SLN Prevent water loss Cosmetic and oral delivery	Docetaxel, Paclitaxel ATRA Curcumin
Nanoemulsion	Oil/water emulsion Kinetically stable Used in parenteral delivery	Curcumin Docetaxel ATRA
Polymeric nanoparticles	Water-soluble, nontoxic, biodegradable Surface modification Specific targeting of cancer cells Ease of reproduction	Paclitaxel Docetaxel ATRA Etoposide
Polymeric micelles	Suitable for water-insoluble drug Biocompatible, self-assembling, Biodegradable, Easy functional modification, Targeting potential	Paclitaxel Docetaxel Camptothecin
Dendrimers	Highly stable, Size easily controlled Easy functional modification	Camptothecin Paclitaxel, Docetaxel
Albumin	Biocompatible, biodegradable, Favourable biodistribution, Enhance tumor uptake of other chemo-drugs	Paclitaxel

3.1.2. Solubility enhancement

Nano-structure delivery system has been widely used to solubilize and deliver poorly water-soluble drug (PWSD). In 2014, Wong and his lab summarized the commonly used nano-delivery systems for PWSD delivery [Narvekar, Mayuri, 2014]. As shown in Table 3-1, various systems can be used for the purpose. Liposome was one of the most commonly used system to solve the problem. It has great potential for surface targeting modification and solubilization. However, liposome particle may have stability issues due to relatively high mobility of the bilayer phospholipid. Also it has been reported to have stability issue when applying filter-based sterilization. In this study, the nanostructured lipid carrier (NLC) will be used for TPL delivery. NLC has advantage of high drug loading, especially with lipophilic drug. As shown in Fig 3-1, basic structure of NLC including lipid core surrounding by single layer of phospholipid with decoration on the surface. Lipophilic API was encapsulated in the core and the phospholipid was stabilized by stabilizer such as cholesterol. NLC can achieve higher encapsulation efficiency due to its solid lipid core with less mobility and relatively stable out layer. The surface of the particle usually decorated with hydrophilic polymer such as poly (ethylene glycol) in order to reduce immunogenicity and escape reticuloendothelial system (RES) to prolong the half-life of the formulation [Peracchia M T, 1999]. The active target ligands conjugated with the long chain hydrophilic molecule will be at the out layer of the particle.

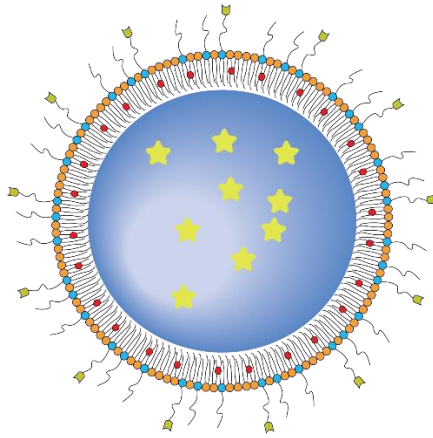


Fig 3-1. Schematic image of NLC with targeting decoration on the surface.

3.1.3. Preparation

Nanoemulsion based nanoparticulate formulation has been widely studied and used in commercial product. As summarized by Neha Gulati and Himanshu Gupta, [Table 3-2](#) summarized the commercially available nanoemulsion product [[Gulati N, 2011](#)]. These FDA approved product indicating the nanoemulsion systems have shown advantages and low safety concerns. The system is transparent or translucent oil in water systems with a mean size around 100-500 nm.

Since TPL can be co-dissolved with the lipid ingredients, the particle system is prepared by self-emulsion technology. All the ingredients are pre-dissolved in water immiscible organic solvent such as methylene chloride, following by water phase added. Then the mixture solution is fully emulsified by high energy input such as sonication or

microfluid technique. During the emulsifying process, the lipophilic phase is surrounded by hydrophilic phase. The amphiphilic phospholipids are at the interaction layer between the two phases, surrounding the lipid core with dissolved API. The solvent in the system was then allowed to evaporate to form stable particle structure. The particles are isotropic mixtures of API, oil, lipid, phospholipid, stabilizer ranging in size from approximately 100 nm. The API remains in the lipophilic core and is protected by the lipid and phospholipid from leaking out to the hydrophilic phase.

Table 3-2. Commercial available product of nanoemulsion formulation

Drug	Brand	Indication
Propofol	Diprivan®	Anesthetic
Dexamethasone	Limethason®	Steroid
Flurbiprofen axetil	Ropion®	Nonsteroidal analgesic
Vitamin A, D, E & K	Vitalipid®	Parenteral nutrition
Palmitate alprostadiol	Liple®	Vasodilator, platelet inhibitor



Fig. 3-2. Product of Diprivan®.

3.2. Alendronate

3.2.1. Introduction

In order to actively targeting the micro-environment of the bone site, scientist has been studied bisphosphonate targeting molecule. Alendronate (ALE), which was one of the most popular agents, has attracted most attention. In 2008, ALE was approved by FDA as a tablet formulation for treatment and prevention of osteoporosis. The high binding affinity with hydroxyapatite, which is the main matrix of bone structure, makes it possible for bone targeting ligand.

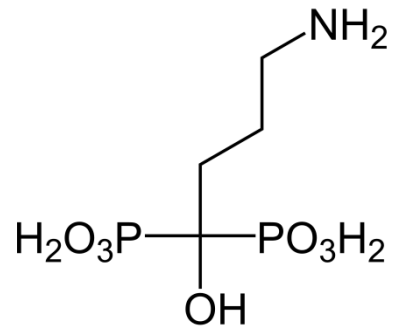


Fig 3-3. Structure of ALE.

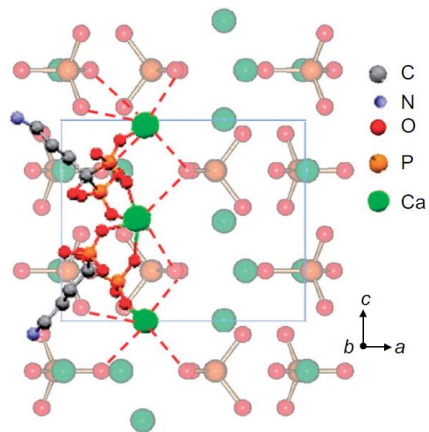


Fig 3-4. Illustrating image of bone matrix with HA and ALE binding route [Boanini E, 2008].

4.2.2. Mechanism of bone targeting

ALE displays a backbone structure of P-C-P, shown in Fig 3-3. The two phosphonate groups are essential for binding to HA [Boanini E, 2008]. As shown in Fig 3-4, the binding was through a tentative interplay between organic and inorganic phosphate in calcium coordination. With incorporating ALE onto NLC, the affinity of ALE with HA will help the particle targeting to the bone matrix. This can enhance the accumulation of active ingredients to the bone tumor site and increase the local concentration. What's more significant, preliminary study done by Pengbo Guo and Wong's lab showed that ALE decorated NP will bind to the bone and stay on site for at least 48 hours without circulating to other organs. After 48 hours injected *i.v.* into rats, particle showed only accumulation to the right leg's bone tissue without spreading to other tissues or bone tissues. This can not only enhance the local concentration at the bone cancer site but can also help minimize the potential systemic toxicity of the potent drug. The ALE targeting on the surface makes it possible to control the toxicity of the TPL, inhibit the osteoclast and kill the breast cancer cells.

4.2.3. Preparation of ALE conjugated phospholipid

As described before, the particle system has a layer of PEG polymer on the surface. In order to decorate the surface with bone targeting agent alendronate, ALE is needed to be pre-conjugated to the PEGylated phospholipid prior to formulation preparation. As reported in previous study, ALE can be conjugated with polymer by

using amine crosslinking reaction with the crosslinker N-hydroxysuccinimide esters (NHS) [Liu P, 2015]. The reaction showed as below.

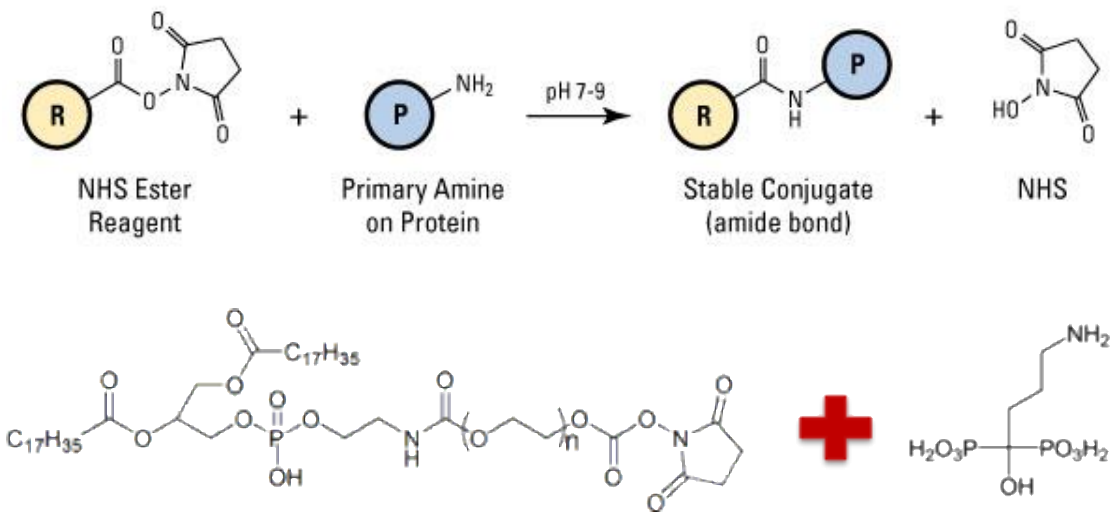


Fig 3-5. Amine crosslink reaction with NHS.

After the reaction, the amine group on the ALE molecule will be substituted with the carboxyl group on the PEGylated phospholipid. Conjugating ALE with DSPE-PEG-NHS yields DSPE-PEG-ALE, which is a phospholipid with ALE decoration on the surface. In this study, different weight percentage of the conjugation was used to test different properties.

3.3 Particle Characterization Techniques

3.3.1. Particle size distribution and surface charge

Particle size distribution is one of the most important properties for all the colloidal delivery system. It can impact particle uptake, absorption, release, biodistribution, elimination, toxicity *et al.* Narrow distribution of the particle usually indicate a well-controlled preparation condition and optimized formulation. In this case, particle size is essential for TPL-NP-ALE distribution at the local site and access to the microenvironment of tumor site. Particle size is measured using dynamic light scattering technique. It can determine the particle size based on the rationale that particle with different size will have different light scattering. Since small and large size molecule alter the light path differently, the intensity peak for the spectra is more realistic and preferred.

Surface charge, on the other hand, is another indispensable parameter nanoparticle formulation. It is dependent on the pKa of the surface group on the particle. Thus, pH condition will be dominant when measuring the zeta potential. For the particle stability,

the ability remain charges on the surface can help stabilize the particles in aqueous environment and prevent it from aggregation. The surface charge sometimes can also influence the interaction between the formulation and the targeted cells or environment.

3.3.2. Encapsulation Efficiency (EE%)

Encapsulation efficiency is another important parameter when designing a colloidal system. It can be calculated by the following equation:

$$\frac{\textit{Amount of drug encapsulated}}{\textit{Total amount of drug added to the system}} \times 100\%$$

EE is a good measurement to optimize the formulation and the preparation process. Moreover, higher EE suggests that the particle system is good for production and financially friendly. The principle to measure EE is to separate the free drug in the solution from the particle system. Several approaches such as filtration, ultracentrifugation, centri-filtration or dialysis can be used. The content of the free drug is usually determined by high performance liquid chromatography (HPLC) or other analytical method such as UV-vis spectrometry.

3.3.3. Morphology

The morphology is a direct way to better understanding the particle matrix structure especially for complicated delivery system such as porous system. Since most nanoparticle system is prepared in suspension, the sample need to be fix in the solution state before observation by microscopy. For system with high melting point excipients (such as polymeric particles), lyophilization of the particle can remove majority of the liquid without jeopardize the matrix. However, since NLC consists lipid core and phospholipids, which has a melting point at or slightly higher than room temperature, fixing the particle can become challenging. Moreover, the lyophilized sample can be melted on the imaging platform due to high energy electron scanning.

Recently a novel EM technology has been extensively studied. Cryo-scanning electronic microscopy (Cryo-SEM), which maintain an ultra-low temperature (-120 °C) during the sample preparation and remain at low temperature during the imaging step. The sample preparation eliminates the transportation of the particles, minimize the possibility of the sample exposing to high temperature. During imaging, ultra-low temperature can maintain sample structure. Although the charges on the sample can cause movement during the electron scanning, by using Cryo-SEM can help the scientist observe materials like NLC the best.

3.3.4. Cytotoxicity study

Before TPL-NP-ALE *in vivo* efficacy study, the cytotoxicity of the system needs to be addressed first. Since the purpose of the project is to design an anti-bone metastasis breast cancer treatment, the toxicity against tumor cells and normal bone cell will be tested. The MTT ((3-(4,5-Dimethylthiazol-2-yl)-2,5-diphenyltetrazolium bromide) assay is an efficient method to examine the cytotoxicity of the treatment at different concentration. NAD(P)H-dependent cellular oxidoreductase enzymes can reducing the MTT dye to its insoluble formazan, which has a purple color. Those enzymes may reflect the number of viable cells presenting in the study.

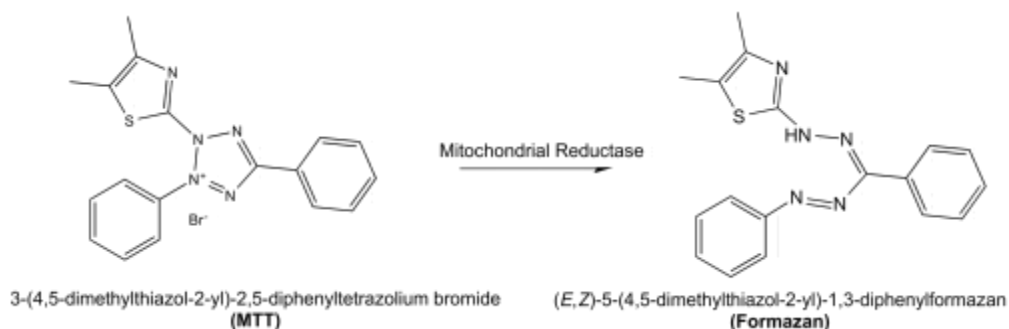


Fig. 3-6. MTT reduction happened in mitochondria of the cells.

However, several limitations of the method may cause inaccuracy of the assay. The MTT reagent has been found to be toxic against some cells, such as eukaryotic [Riss TL, 2013]. This may influence the real cytotoxicity of the treatment. On the other hand, due to the principle of the measurement, the tetrazolium reduction reaction reflects the cell metabolism of the enzyme in the mitochondria. Under certain circumstances, the metabolism reflects the cell viability. However, the measurement does not illustrate the cell number. The rate of the MTT reduction can be changed with culture conditions and the physiological state of the cells. For instance, cell metabolism is significant faster when it growing as a monolayer than those under confluent condition.

In addition to the MTT assay, clonogenic assay will be used to further study the proliferation of the cells under different treatment and concentration. The assay measures the colony forming efficiency and the colony number will be measured.

MDA-MB-231 will be used as a model aggressive breast cancer cell for the anti-cancer efficacy. MC3T3 will be used as normal bone cell model for the toxicity study.

3.3.5 Stability

The stability of the TPL-NP-ALE system also needs to be clarified before further study. Different condition should be tested in order to simulate real storage or biological condition. Firstly, the storage condition for the suspension at room temperature will be examined. Secondly, the TPL-NP-ALE is supposed to be stable under biological environment such as plasma or extracellular fluid, which include growth factor and other ingredients. Thirdly, since most particle formulation will be lyophilized and stored, the stability of the freeze-dried sample also need to be studied. Particle size distribution and surface charge will be used as indicator of the stability of the particle.

CHAPTER 4. OBJECTIVES OF THE STUDY

Specific Aim 1: Develop and characterize an optimized alendronate-targeting nano-structured lipid carrier to encapsulate TPL.

Hypothesis:

High TPL encapsulating and stable formulation with NP-ALE system. The formulation can not only show great affinity to the bone matrix but can also achieve sustained release with TPL.

Specific Aim 2: Compare free drug and TPL encapsulated in particle *in vitro* with breast cancer cell lines. Evaluate the toxicity with normal bone cell lines.

Hypothesis:

TPL nanoparticle formulation can achieve better cytotoxicity with cancer cell lines while stay low toxicity with normal osteoclast.

Specific Aim 3: Examine the *ex vivo* performance of TPL-NP-ALE with bone.

Hypothesis:

TPL-NP-ALE has high binding efficacy with bone tissues.

CHAPTER 5. EXPERIMENTAL SECTION

5.1 Materials

Triptolide (Cat No.: 38748-32-2) and Docosahexaenoic acid (Cat No.: 6217-54-5) were purchased from Cayman Chemical (Ann Arbor, USA). Tripalmitin was obtained from TCI, Inc. (Tokyo, Japan). Phospholipids were obtained from Avanti Polar Lipids, Inc. (Alabaster, USA). Dichloromethane (DCM), Tween 80, acetonitrile, hydrochloride acid, acetic acid was all purchased from Fisher Scientific (St. Louis, USA).

5.2. Preparation of Triptolide nanoparticle (TPL-NP)

TPL-NPs were prepared using emulsification solvent-evaporation method. Lipid and oil ingredients were mixed with TPL and the mixture was dissolved in dichloromethane. The organic phase was emulsified in biotech water with the ratio of organic phase to aqueous phase approximately equal to 1:10. The mixture was vortexed for 30 seconds, sonicated in sonication bath (Branson 2800, sonication mode at room temperature of 25 °C) for 1 minute to allow fully emulsifying, followed by another 4 minutes sonication to evaporate majority of the organic solvent. The solution was stirred at room temperature for 6 hours.



Fig. 5-1, Bath sonicator. Branson 2800

The emulsifying step during the preparation can also use microfluidic technology (not used in this study). The microfluid method has been extensively studied and used in upstream scaling up for emulsion-based formulation. Different principles have been used depending on different formulation design. An example has been shown in [Fig. 5-2](#). Two phases (e.g. oil and water) were fed from the left of the chip and mixed at the intersection of the line. By controlling the flow speed, the system can achieve high shear force that emulsify the droplet into desired size range. The turning area of the path allowed the organic solvent in the droplet to evaporate, collecting the final product at the end. The microfluid technology has advantages such as great size distribution control, module like structure, easy to handle. The design of the chip allow to scale up by parallely increasing the chip number to achieve exact same condition.

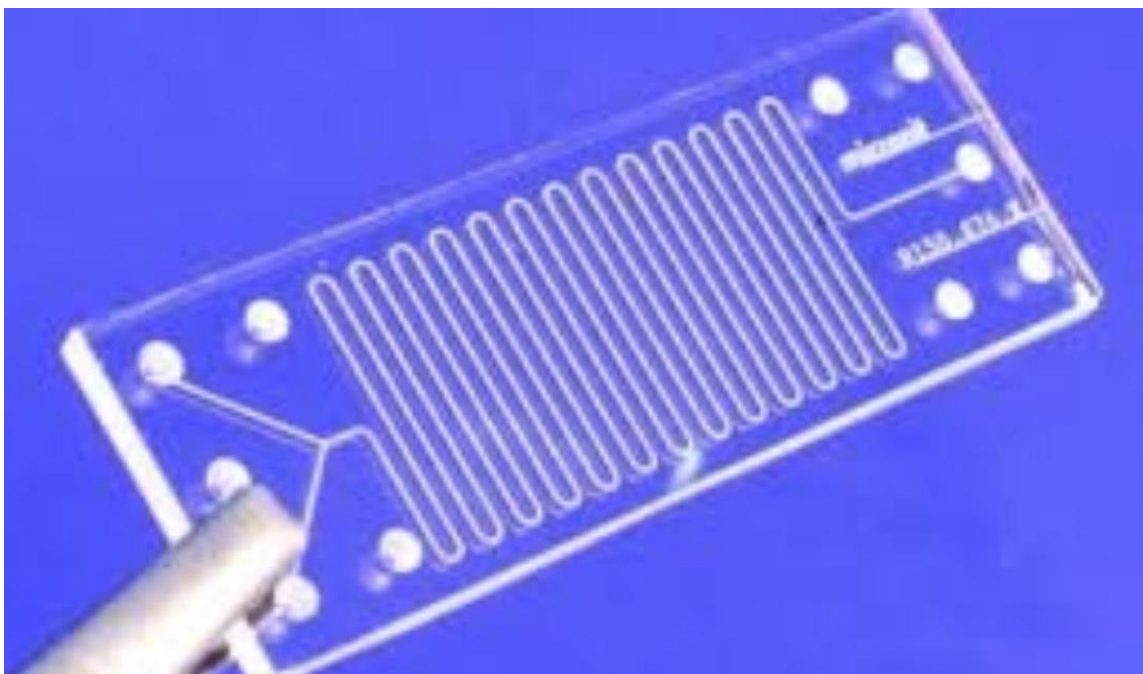


Fig. 5-2. Example of microfluid chip design.

5.3. Preparation of alendronate conjugated phospholipid

DSPE-PEG-NHS powder was dissolved in alendronate (ALN) solution (molar ratio of DSPE-PEG-NHS: ALN=1:5) in HEPES buffer (pH=7.8) to initiate NHS ester crosslinking reaction [Hermanson G T, 2013]. The resulting mixture was gently stirred at room temperature for 2 h, and then dialyzed (MWCO 1kDa, G-Biosciences, St. Louis, MO, USA) at room temperature for 24 h to remove unreacted alendronate. The solution containing the DSPE-PEG-ALN was lyophilized into powder form for nanoparticle preparation.

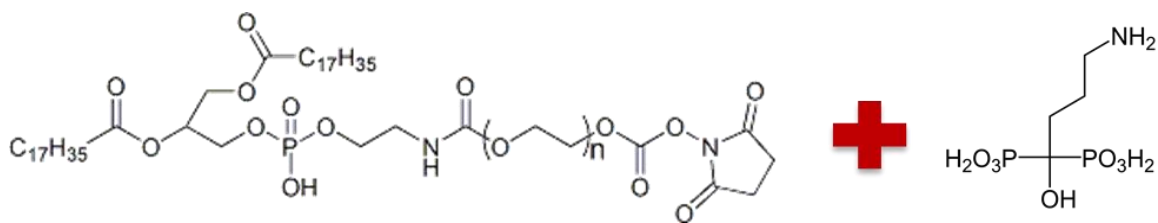


Fig. 5-3. Alendronate conjugation amine crosslinking reaction with DSPE-PEG-NHS.

5.4. Preparation of alendronate decorated triptolide nanoparticle (TPL-NP-ALE)

In order to enhance the bone targeting specificity, ALE-PEG-DSPE was used to decorate the nanoparticle formulation. The process of preparing TPL-NP-ALE was similar to the non-decorated one, except given weight percentage of ALE-PEG-DSPE was used based on the study during the preparation process

5.5. Characterization of TPL-NP

5.5.1. Particle size distribution and surface charge

The size distribution, polydispersity index (PDI) and zeta potential of TPL-NP and TPL-NP-ALE were measured by photon correlation spectroscopy using Zetasizer® 3000HS (Malvern, UK). For size distribution and PDI measurement, 25 μ L sample suspension was diluted in 1.0 mL distilled water. On the other hand, same sample preparation was used for zeta potential analysis. Fifteen successive cycles were run for the measurement for each sample. Size data were presented based on the distribution by intensity.



Fig. 5-4. Zetasizer® 3000HS

5.5.2. Stability

Selected samples of TPL-NP and TPL-NP-ALE formulation were kept under 25 °C and 37 °C for 14 days under aqueous or bio simulated environment (media with growth factor). The size and particle surface charge were measured to evaluate the physical stability under storage and biological environment.

5.5.3. Encapsulation Efficiency for TPL formulation

The encapsulation efficiency (EE) of TPL formulation was determined by ultra-centrifugation separation. The sample suspension was centrifuged at 2,500 g at 4 °C for 30 min using Centriprep® centrifugal filters with 3,000 Dalton molecular weight cut off. The supernatant was then transferred to a volumetric bottle and brought up to the volume by DDI water. The sample was analyzed for TPL content using RP-HPLC described below.



Fig. 5-5. Centriprep® centrifugal filter

Table 5-1. HPLC method for TPL.

Column	X-Bridge C18 100 mm 5 μm
Temp	30 °C
Mobile Phase A	Water w/0.05 % TFA
Mobile Phase B	Methanol:Acetonitrile 50:50 W/ 0.05 % TFA
Flow Rate	1 mL/min
Gradient	
0 min	10% B
2 min	10% B
10 min	45% B
21 min	95% B
23 min	95% B
23.01 min	10% B
25 min	10% B
Run Time	25 min
Detector	Diode Array UV-Vis
Wavelength	218 nm
Injection Volume	10 or 70 μ L

5.5.4. Hydroxyapatite affinity study

TPL-NP-ALE was prepared incorporate with red dye phospholipid. The hydroxyapatite (HA) powder was dispersed at 10 mg/mL concentration in phosphate buffered saline (PBS). The TPL-NP-ALE was added to the suspension and shake at room temperature for 1 hour. Then the samples were centrifuged at 3000 rpm for 5 min to separate the powder from the suspension. The supernatant was analyzed by UV/vis at 337 nm to determine the binding efficiency.

5.5.5 Drug releasing study

TPL NP formulations were tested for drug releasing profile to compare with the free drug. The study was done by using dialysis dissolution method. 15 kDa molecular weight cut off membrane was used to separate released drug from the formulation. The releasing study was evaluated against Phosphate Buffered Saline (PBS) with 0.1% Tween 80. Tween 80 was presented to prevent the drug from attaching to the plastic dialysis tube. The formulation was transferred into the dialysis tube after the preparation. The tube was then put into 35 mL PBS drug releasing media and the system was stirred at 37 °C. At predetermined time point, 200 µL sample was taken from the media outside the dialysis bag. The sample was then analyzed by HPLC method listed in [Table 5-1](#).

5.5.6. Morphology

The morphology of the particle formulations was observed by using Hitachi S4700 scanning electron microscope. The experiment was done in University of Delaware Bioimaging Center. The microscope was equipped with a Gatan Alto 2500 cryo-system. After preparing the particles, samples were first filtered through 0.01 µm carbonate filter to remove majority of water. Filter paper with particles was then transfer and fix onto the sample platform. Then samples were plunged into liquid nitrogen slush and a vacuum was pulled allowing sample transfer to the Gatan Alto 2500 cryo chamber at a temperature of -120 °C. Samples were sublimated for 10 minutes at -90 °C to

remove loosely bind water, followed by cooling to -120 °C again. A thin layer of Gold Palladium coating was sputtered onto the samples. The samples were then transferred into a Hitachi S-4700 Field-Emission Scanning Electron Microscope for imaging.



Fig. 5-6. Hitachi S4700 Scanning Electron Microscope with Gatan Alto 2500 cryo-system.



Fig. 5-7. Filters with sample were fixed onto the sample platform, coated with gold platinum.

5.5.7 Cytotoxicity study

MTT Cell viability assay

MTT assay was used to evaluate the formulation cytotoxicity against various cancer type cell lines. After preliminary test with cell lines and triptolide, optimized condition was chosen. The 96-well plate was seeded with 8000 cells/well in 200 μ L/well media and incubated for 24 hours. Next, original media was removed and the cells were treated with drug and particles. After incubating for 24 hours with the treatment, media containing drug or particles were removed and fresh media was refilled with 200 μ L/well,

incubate for another 72 hours. As described in the background, triptolide has effects on the cell cycle arrest and lead to apoptosis, the cytotoxicity of the drug may have a delayed effect on the cancer cells. Thus the 72-hour recovery time will allow the remaining drug effect to be observed and better reflect the real situation. After the incubation, 20 μL /well 0.5 % MTT solution was added into the plate and incubate another 2 hours to have MTT reduction reaction by the cells.

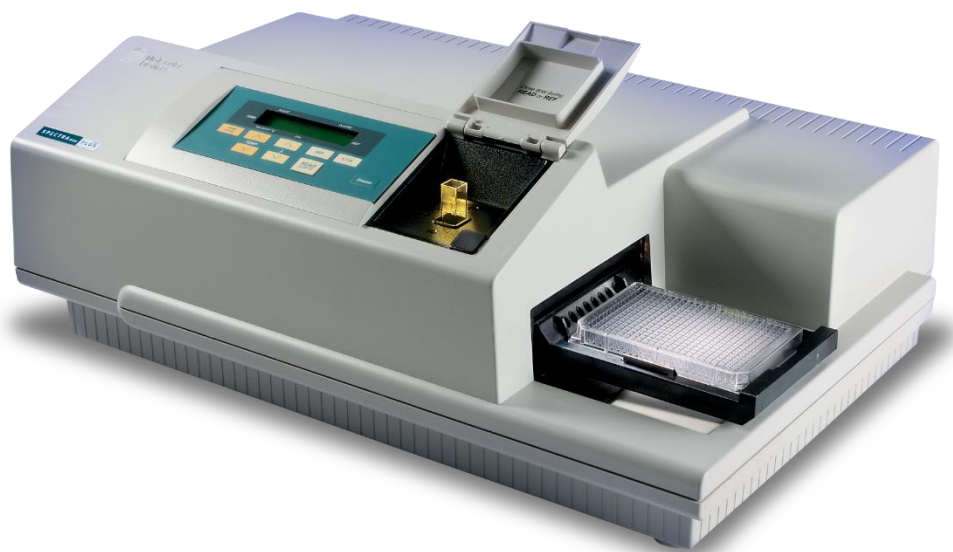


Fig. 5-8. SpectraMax plate reader.

After coloring the metabolizing cells by MTT reduction reaction, the liquid was poured out from the plate and 150 μ L/well DMSO was added to re-suspend the wells. The plate was read of UV absorption at wavelength of 590 nm and 620 nm with SpectraMax M2 at room temperature at 25°C. The reading at the wavelength of 620nm was served as a reference reading.

Clonogenic assay

Clonogenic assay was used in addition to MTT for direct toxicity observation. MC3T3 cell was distributed as 400 cell/dish into the 6-cm culture dishes in drug-free culture medium at standard cell culture conditions for 1 days. After the cells were attaching to the bottom of the dishes, media was removed and the cells were treated directly with media solution containing drug concentration shown in the following table. With 1-day treatment, the media was removed and replaced with fresh media to let the cell recover and form colonies. After 12 days recovery, the colonies were fixed and stained with 0.5% solution of methylene blue in methanol and the numbers counted. Cell survival of each treatment was calculated as $(\text{number of colonies formed} \times 100\%) / (\text{number of cells plated})$.

Table 5-2. Drug formulation used in clonogenic assay.

Plate	1	2	3	4	5	6
5 nM	Free	Blank	TPL-NP	4%	6%	8%
20 nM	Drug	NP	w/o ALE	ALE-NP-TPL	ALE-NP-TPL	ALE-NP-TPL

5.5.8 Cell uptake study

In order to compare the formulation uptake differences between cancer cells and normal cells, a fluorescence technique will be used to observe the formulation uptake of the cells. In this study, MC3T3 and MDA-MB-231 cell lines were used as normal cell and cancer cell model, respectively. Red phospholipid dye was incorporated into the regular particle formulations for microscopic observation. Based on previous *in vitro* study, 6% ALE-NP was used as the therapeutic formulation. Since TPL was relatively potent, cells treated with the formulation with API will result in cell death. Thus, blank particle formulation will be used for this study.

The cover slips were sterilized and treated with poly-l-lysine to coat the surface for better cell adhesion. 6 treated coverslips were put into 10 cm cell culture dish and seeded with different cell lines. After one day incubation, each coverslip was transfer into 3 cm dish and treated with 2 mL 0.25 mg/mL 6% ALE-NP without triptolide. After 3.5 hours treatment, 2 μ L Dapi dye was added into each dish to dye the nucleus. After another 0.5 hour, the coverslips were ready for the slide's preparation.

After the treatment, the media was replaced with 2 mL PBS buffer to wash away the remaining dye. After 2 min, the PBS was removed and 2 mL 2% formaldehyde solution was added into the dish for 2 min to fix the cells. After the fixing, the coverslip was washed again and put on the slide glass. If not observing immediately, the coverslip would be sealed in order to prevent drying. The images were further modified and overlaid by using ImageJ software.

5.5.9. Anti-migration test

In order to better understand the anti-migration effect of TPL free drug, a scratch wound assay was used. PC3M aggressive metastatic prostate cancer cell line was used to create the most harass environment. The cells were seeded into 30-mm cell dishes and allowing to grow overnight to achieve confluency greater than 75%. This allow the cells to almost form a single layer on the bottom. If the confluency achieves 100% before the test, the cell metabolism and proliferation may slow down, causing inaccuracy to the study. Then the monolayers were carefully wounded by using a 200 μ L sterilized pipette tip and the treatments were added to the plate. At pre-determined timepoints, dishes were imaged by using an optical microscopy.

CHAPTER 6. RESULTS AND DISCUSSION

6.1. Particle Characterization

6.1.1. Lipid selection

Although TPL molecule has a relatively low aqueous solubility (14 $\mu\text{g/mL}$), the LogP of the molecule is not quite optimistic. As reported in previous paper, TPL only have 0.6-0.8 partition coefficient value with several most used solid lipids [Zhang C, 2014]. This may cause TPL leaking out from the lipid core of the particle system, result in a low EE. Thus, the first step of the particle design was to have a proper lipid selection that is suitable to dissolve TPL molecule.

Docosahexaenoic acid (DHA, shown in Fig. 6-1.) has drawn increasing attention recently for its outstanding capacity for API dissolving. On the other hand, DHA has been reported to have anti-cancer effect (Fig. 6-2.). In this study, DHA was compared with commonly used solid lipid triolein oil. Besides, tripalmitin was used in all the formulation as another solid lipid ingredients.

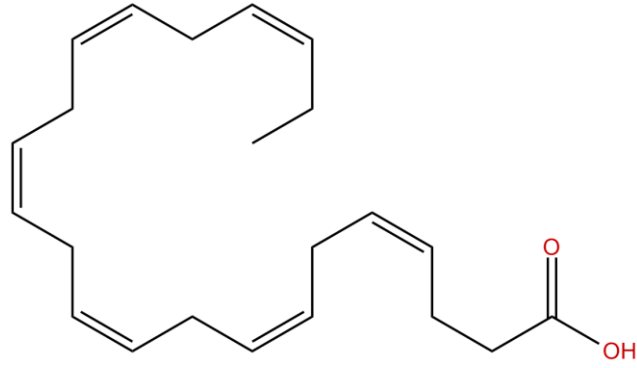


Fig. 6-1. Structure of Docosahexaenoic acid (DHA).

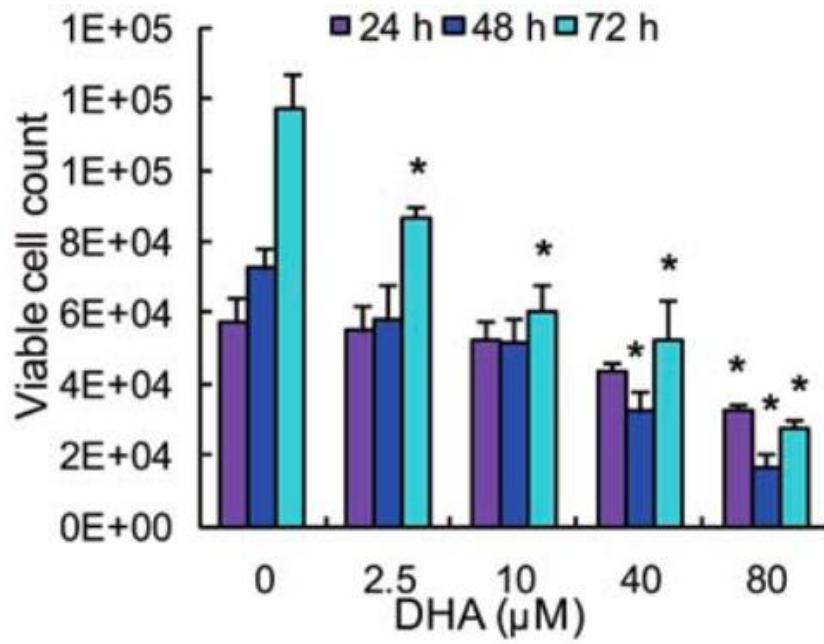


Fig. 6-2. DHA anti-cancer effect with BxPc3-RFP pancreatic cancer cell line.

Table 6-1 shows the study design of the lipid selection. Particles were prepared with different lipid content and tested for the stability regarding size distribution in both water and biological simulated condition. All the formulations maintained the sample total lipid content (weight percentage). The results of the size stability are shown in Fig 6-3.

Among all the formulation, F5 showed the best stability with size remain constant around 100 nm for 10 days under both conditions. All triolein oil formulations had significant aggregation after few days showing as size increase. The DHA group showed relatively stable results at room temperature. Most formulation stayed relatively stable at bio-simulated condition except formulation 6. Considering 100 nm targeted particle size, F5 will be used for the following studies.

Table 6-1. Lipid selection study design.

Test Group	Content %W/W in Dry Form		
	<i>Triolein Oil</i>	<i>DHA</i>	<i>Tripalmitin</i>
Formulation 1	10	-	22
Formulation 2	15	-	17
Formulation 3	20	-	12
Formulation 4	-	10	22
Formulation 5	-	15	17
Formulation 6	-	20	12

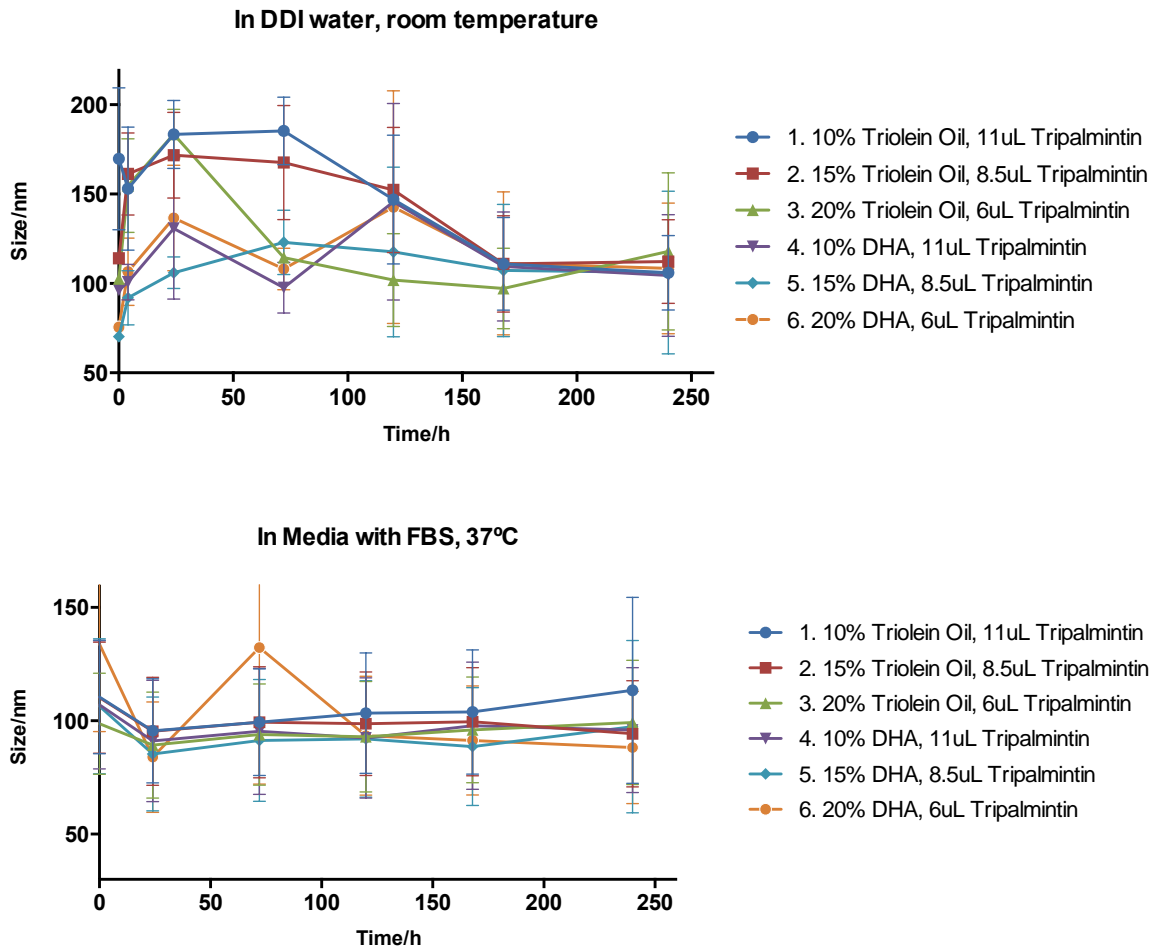


Fig 6-3. Size stability study for lipid selection.

7.1.2 Drug load study

Based on the previous study, 15% DHA formulation (F5) was found to be the most suitable formulation for TPL encapsulating. On the other hand, different drug load was further tested to achieve higher drug loading efficiency. The formulation designs

were shown in [Table 6-2](#). As F5 was prepared with 5% drug load, 7.5 and 10% formulations were studied and compared with F5. Size distribution and encapsulation efficiency were tested. EE was an essential property which illustrated the capability of the formulation encapsulating the API. The results were shown in [Fig 6-4](#).

Size distribution of the formulation after preparation was not significantly different between three formulations. All formulations had size around 100 nm. On the contrary, EE is significantly different as 5% drug load can achieve as high as 97% while higher drug load can only achieve EE lower than 50%. This may cause by the solubility of the API in DHA oil. Based on the results, only 5% formulation was considered as successful encapsulating of the API. In spite of this, 5% drug load of TPL is sufficient enough for the cancer treatment as shown in later section, TPL is a highly potent compound and the dose of the drug is relatively low. Thus, F5 was chosen to be used for further studies.

Table 6-2. Formulation design for drug load study.

	Triptolide/ μg	Drug Load
Formulation 5	250	5%
Formulation 7	375	7.5%
Formulation 8	500	10%

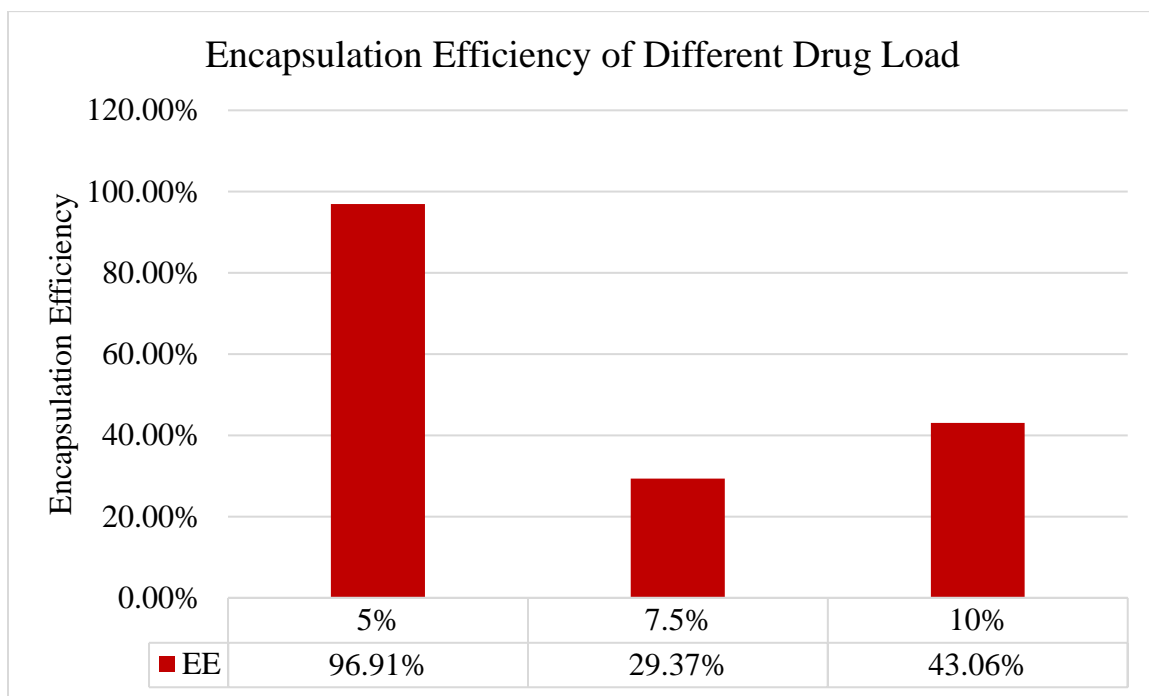
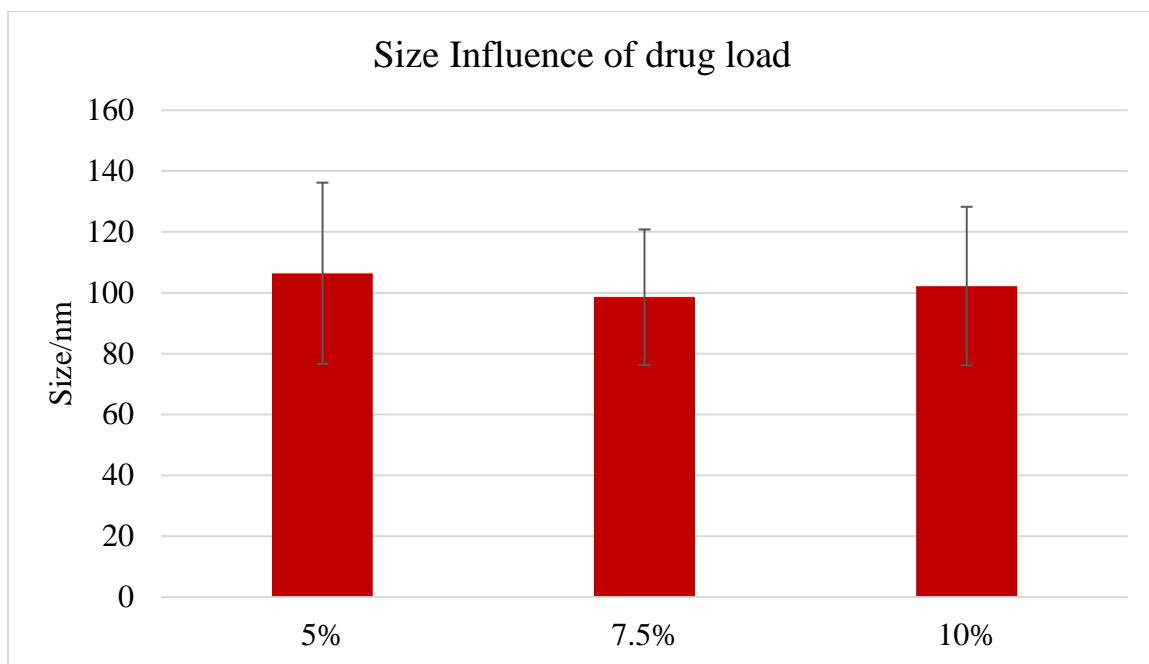


Fig 6-4. Size and EE of different drug load formulation.

6.1.3. ALE decorated NP

After having an optimized formulation, alendronate was incorporated into the delivery system. Method for preparing ALE conjugated phospholipid was described in section 6.3. Five different formulations were designed and tested for the ALE phospholipid incorporating, shown as [Table 6-3](#). The total amount of the ALE phospholipid and mPEG-DSPE was kept the same. Formulations were test for the size and surface charge stability under 25 °C storage condition and 37 °C biological condition. The result is shown in [Fig 6-5, 6-6](#).

All the formulations were able to achieve relatively stable without dramatically size change under storage condition. On the other hand, all formulations shrink about 30 nm after added to the bio-simulated media. This may cause by the surface of the particle due to the alteration of the surface charge by the buffer system, illustrated in [Fig 6-6](#). Generally speaking, F8, 9, 10 (4, 6, 8 % ALE) showed better size property and stability among all the formulation with the targeted size no larger than 100 nm. F9 showed less stable properties regarding the surface charge.

Table 6-3. Study designed for ALE decorating.

Test Group	Content %W/W in Dry Form	
	ALE-PEG-DSPE	mPEG-DSPE
Formulation 5	0	32.5
Formulation 7	1	31.5
Formulation 8	2	30.5
Formulation 9	4	28.5
Formulation 10	6	26.5
Formulation 11	8	24.5

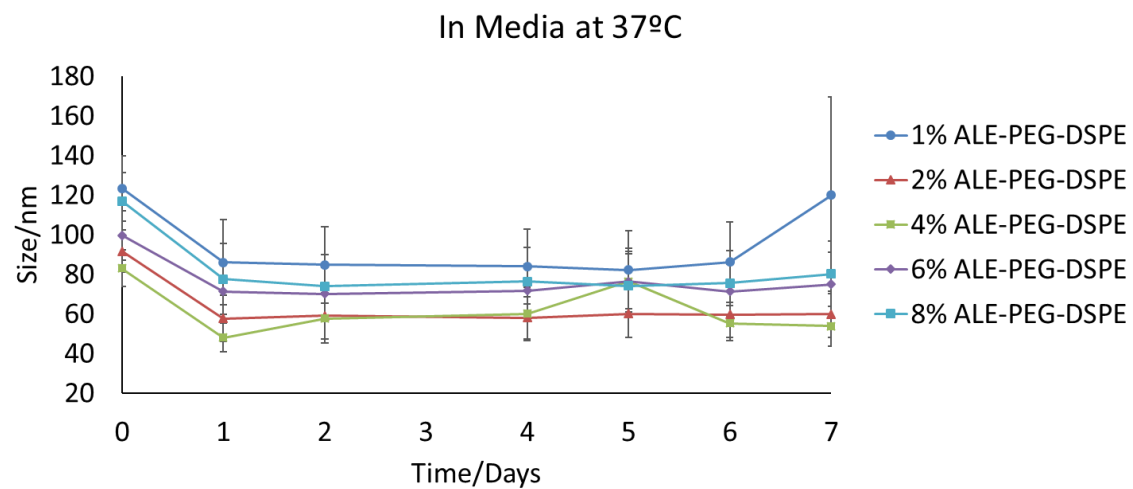
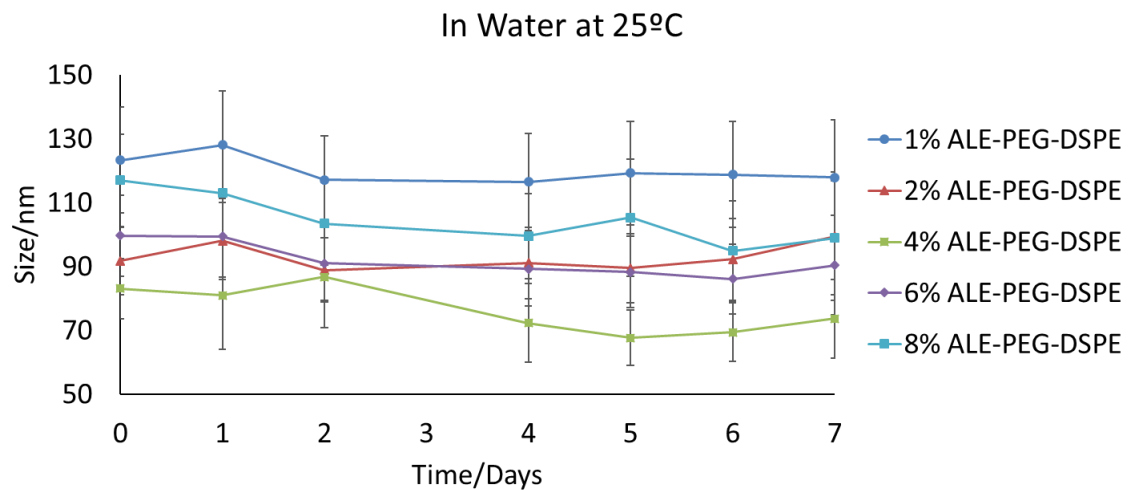


Fig 6-5. Size stability study for ALE decorating formulation.

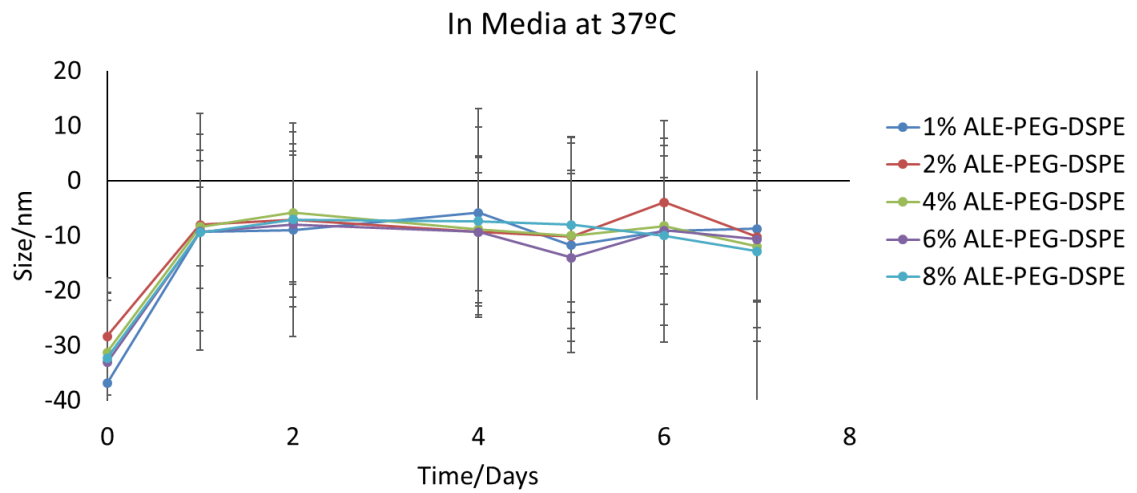
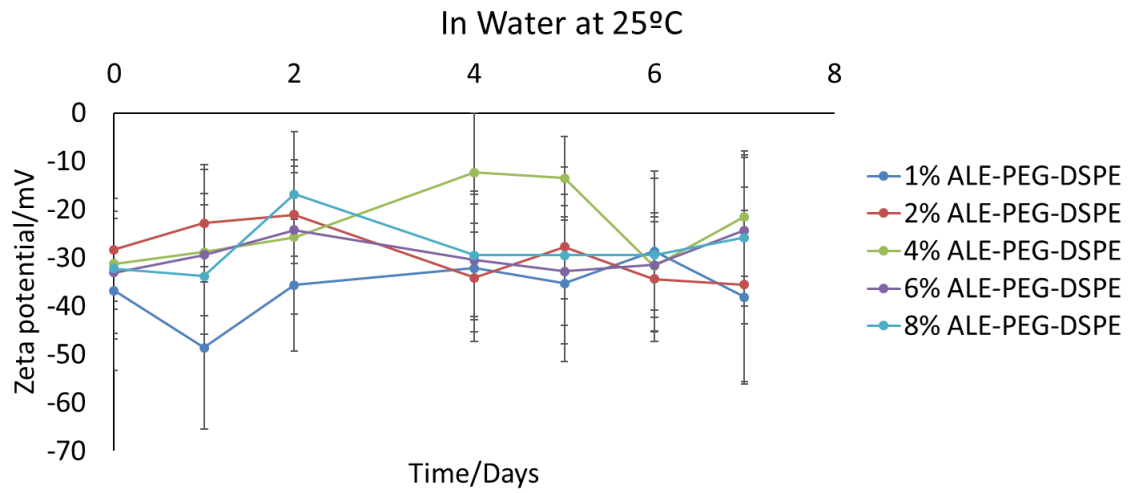


Fig 6-6. Surface charge stability for ALE decorating formulation.

6.1.4. Encapsulation Efficiency

Based on the stability results, F5, 8, 9, 10 were tested for EE. As indicating before, EE is considering important properties that illustrated the capability of the formulation encapsulating the API. As shown in Fig. 6-7, all the formulation has achieved a more than 95 % EE. What's more, for the ALE decorated group, the EE increased for 3% compared with the undecorated particles. This may result from the stability effect of ALE on the surface of the particle that prevent the API from leaking out after the preparation. All in all, the formulation can achieve a relatively high EE, indicating the excellent API loading capability.

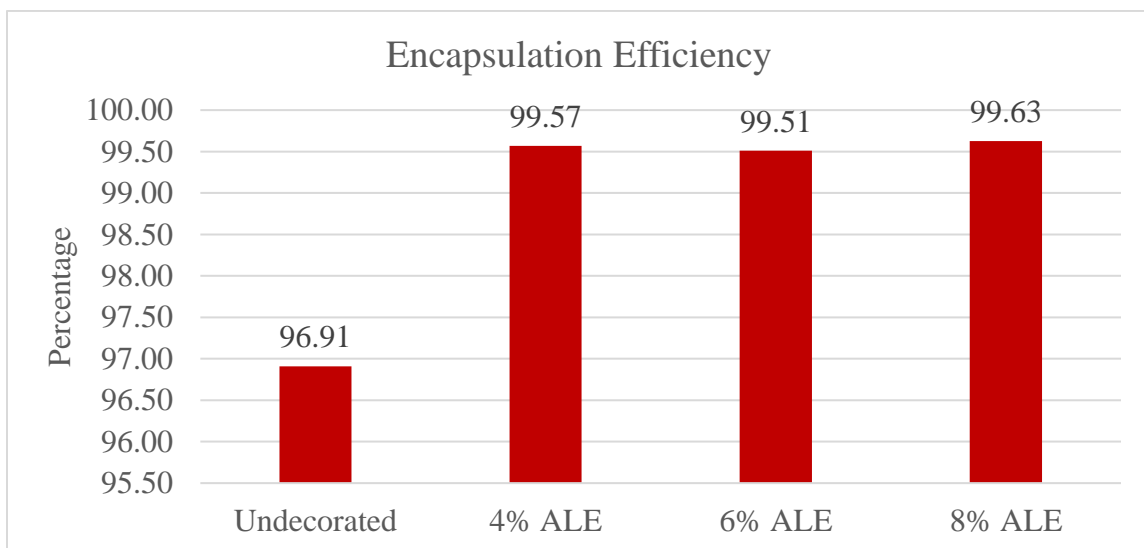


Fig 6-7. Encapsulation efficiency study for F5, 8, 9, 10.

6.1.5. Differential scanning calorimetry (DSC)

To further confirm the crystallinity of the API in the particle system, DSC technique was used to test the thermal properties of the sample. The TPL-NP without ALE decoration and blank particle were tested in this study. The sample was freeze-dried after preparation at -50 °C for 24 hours to remove water content. 3 mg samples were weighted into micro pan. Since the lipid will melt during the heating procedure and the particle structure will be interrupt, single heating cycle was tested. The results are shown in [Fig. 6-8](#).

At around 40 °C, both samples have shown endothermal peak, indicating the melting area for low melting point lipid ingredients in the system. As the temperature rising, huge endothermal step followed by several small melting peaks was observed. This is caused by the melting or chain relaxation of the phospholipid and the polymer conjugation. As reported before, TPL API has melting point at 226 °C. There is no endothermal peak around this temperature range for TPL-NP sample, suggesting that the API was well dissolving in the lipid core of the particle, staying as amorphous state. The DSC results confirms from another aspect that the particle formulation has outstanding capability of encapsulating TPL into the matrix.

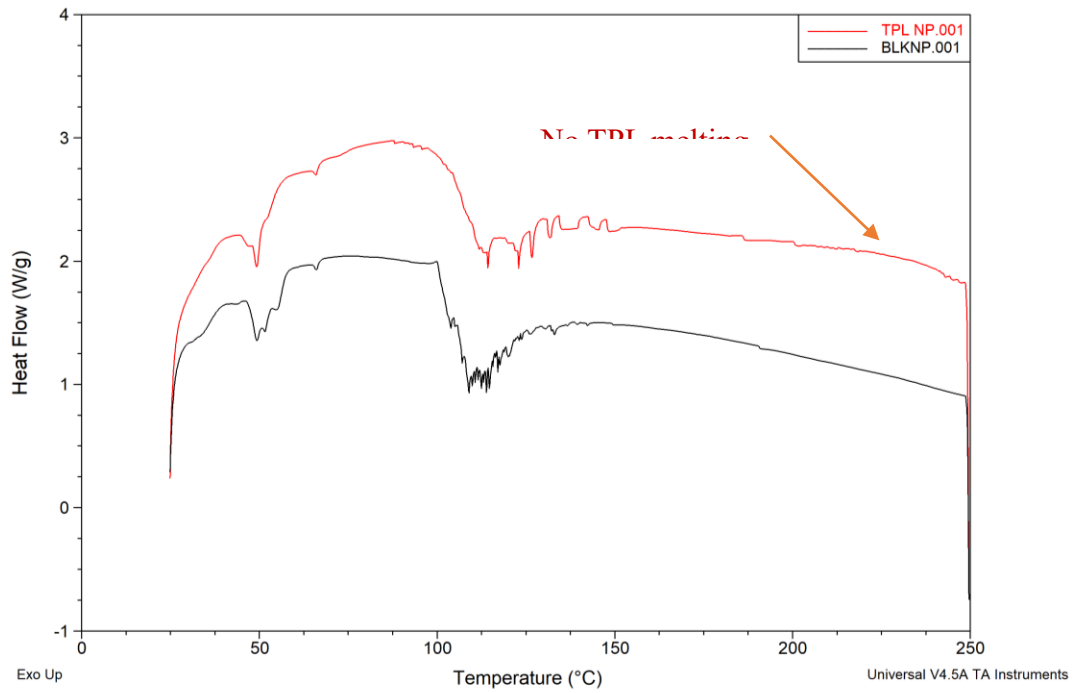


Fig. 6-8. DSC graph for blank particle and TPL-NP without ALE decoration.

6.1.6. Hydroxyapatite affinity study

Before moving to animal study, the bone binding efficacy of the formulation needed to be tested to confirm the hypothesis. Hydroxyapatite, the main component of the bone mineral, was used as a substrate representing bone tissues in *ex vivo* study. Fig 6-9, 6-10. showed the results and the image of the affinity study. With the increasing of the ALE amount, the affinity of the particles to HA powder increased significant. What's more, with the increasing from 1% to 2%, the binding efficiency went up significantly, for almost 3-fold. Between 2% and 8%, the increase of the binding rate showed a linear relationship with the ALE amount. The photo also showed similar trend, with more ALE resulting in more red powder. The results not only proved the bone binding efficacy of the formulation, but also illustrated the relationship between the ALE amount and the binding rate.

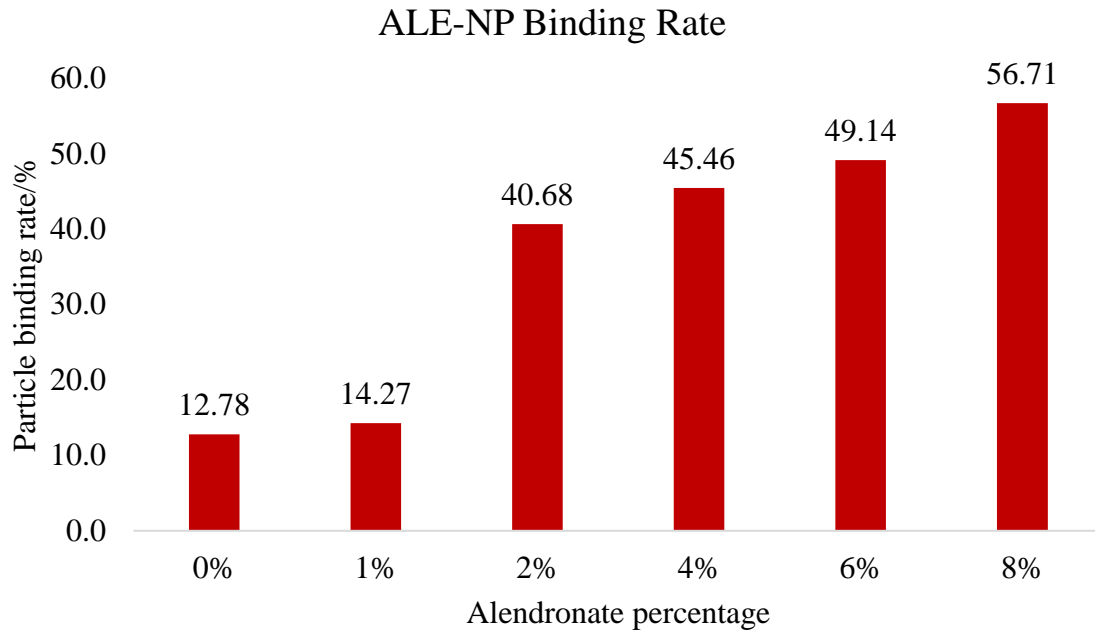


Fig 6-9. Binding efficiency study.

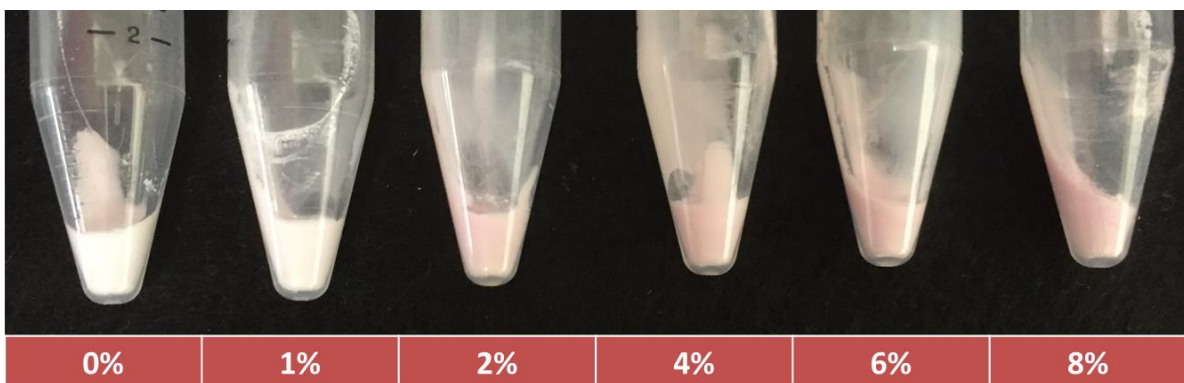


Fig 6-10. Photo image of TPL-NP-ALE binding HA powder.

6.1.7. Drug releasing study

As the optimized ALE particle formulation has been discovered, the drug releasing of the NP needed to be tested. Ideal particle formulation should have a minimal burst release, sustained release and close to 100% drug recovery. For nanoparticle drug releasing, dialysis technique is commonly used to separate the released drug molecule with the formulation. The molecular weight cut up should be at least 10 times higher than the API molecular weight to ensure efficient membrane cross.

The results are shown in [Fig. 6-11](#). Free TPL was pre-dissolved in DMSO as solubilized vehicle. It showed 100% releasing membrane in 1 hour. This speed is limited by the membrane crossing efficiency of TPL. On the other hand, all particle formulation showed sustained release with close to 100% release in 6 hours. Formulation without ALE decoration showed burst release at the first 0.5 h while all the ALE NP formulation had significant less burst release effect. This is a great advantage of the ALE formulation compared with the undecorated one. Group with 4% decoration showed the slowest release while 8% ALE formulation showed the fastest releasing profile.

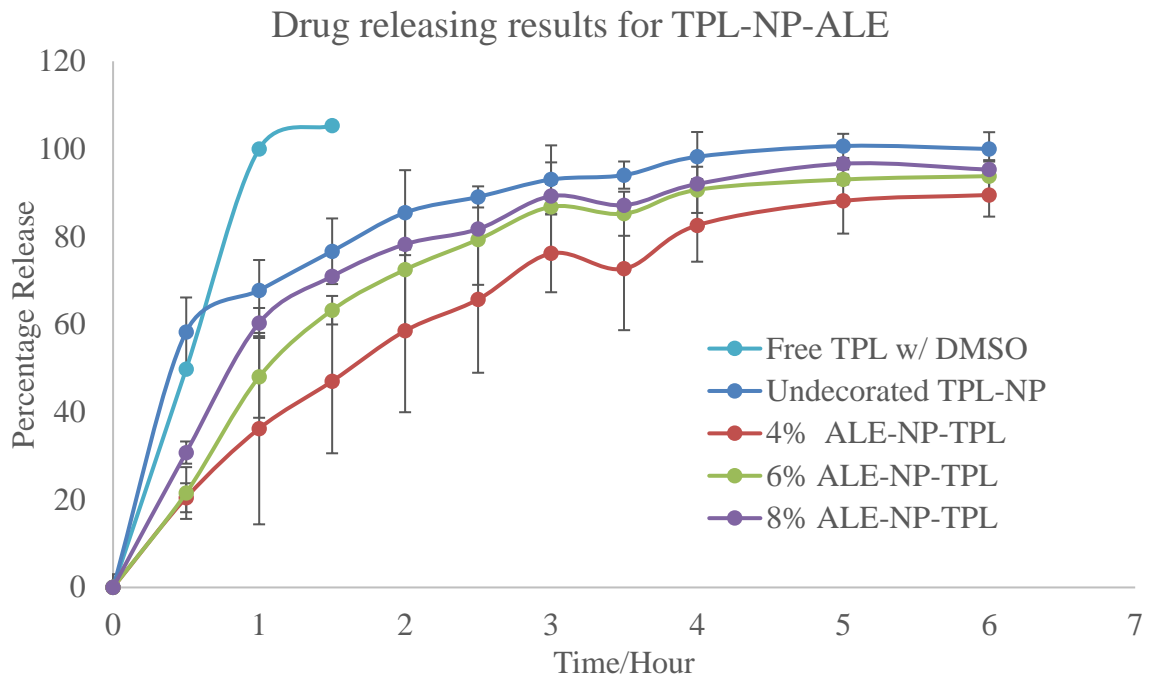


Fig. 6-11. Drug releasing profile for different formulations.

6.1.8. Morphology

The morphology was observed by using cryo-SEM technology. Since the particle consists some low melting point lipid, regular SEM for the lyophilized samples are challenging. Samples were observed melting during the sample preparation step or under high energy electron beam scanning. Thus, keeping the sample at -120 °C before and during imaging can help the particle maintaining the structure. The results are shown in [Fig. 6-12](#).

As shown in Fig. B, particles were shown to remain at around 90 nm. This may due to the fact that the freezing of the sample causing the particle shrinking in size. In spite of this, the particles were found to have relatively uniform distribution. Fig. A showed large magnify images, indicating that sample was not uniformly distributing on the sample platform. This caused great challenging during the focusing and capturing of the photos, as particle with surface charges would move around or form aggregation. Sample preparation technique has potential to be optimized for better images.

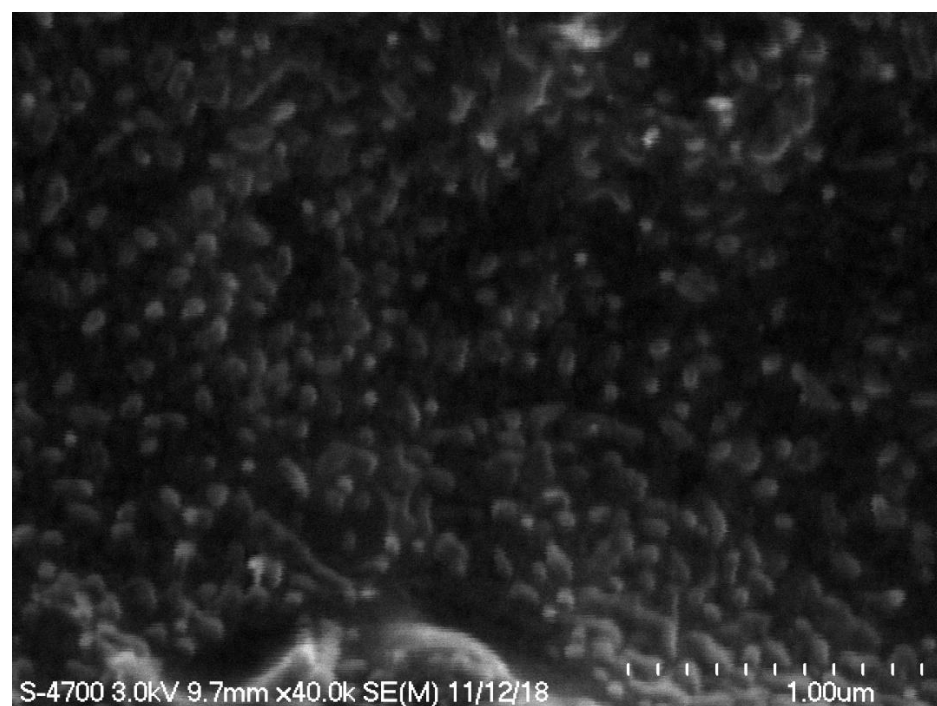
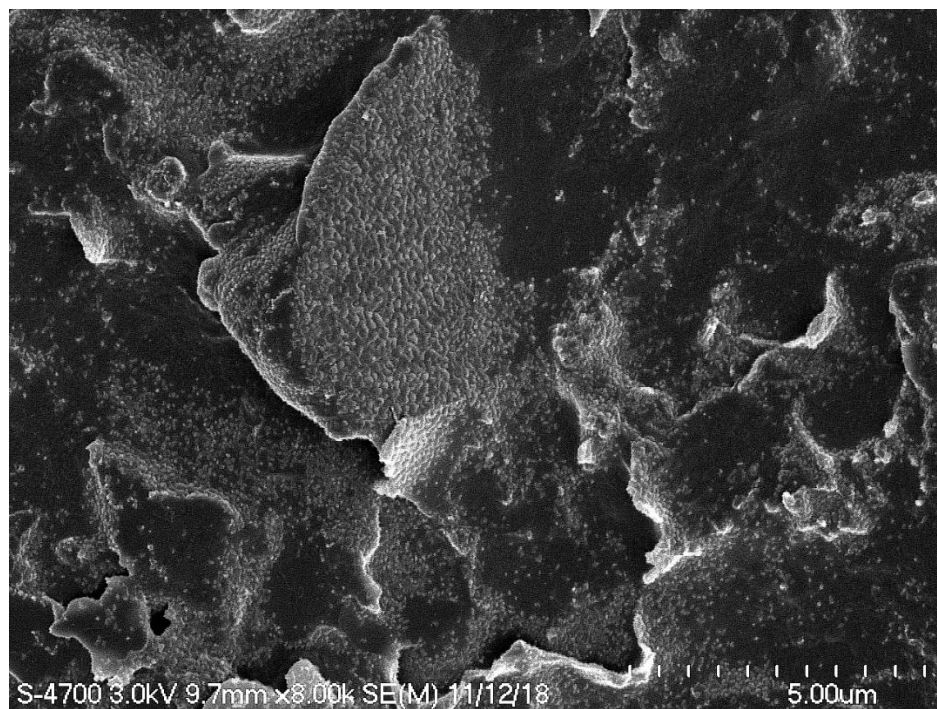


Fig. 6-12. Cryo-SEM images of TPL-NP.

6.2. *In Vitro* cell study.

Before animal tests, *in vitro* cell works are great tool for proof of concept study and preliminary research for efficacy, toxicity and uptake of the formulation. In this study, various types of cancer cell lines were used to demonstrate the anti-cancer effect of TPL and TPL loaded formulation. Specifically, MDA-MB-231 cell line was used as aggressive breast cancer cell model. MDA-MB-231 is human epithelial breast cancer cell lines that established from a 51-year-old female with metastatic mammary adenocarcinoma. The cells are highly aggressive, invasive and poorly differentiated triple-negative breast cancer (TNBC, estrogen receptor, progesterone receptor, human epidermal growth factor receptor 2 negative). On the other hand, MC3T3-E1 cell line was used as a normal bone tissue cells for the toxicity study. The cell line was preosteoblast derivative from mouse bone tissue.

6.2.1. Anti-cancer efficacy study

8 cell lines were used to test the anti-cancer cytotoxicity of TPL-NP against various types of cancer. MTT assay was used for the screening study. The results are shown in [Fig. 6-13](#).

TPL free drug and TPL-NP showed great anti-cancer effect with IC₅₀ ranging from 20-50 nM depending on different cell lines with different cancer type. For the most

aggressive cell line PC3-M, proliferation has been enhanced at relatively low concentration. This may be due to the natural selection with low concentration at cellular level. The NP formulation has the similar or slightly enhanced cytotoxicity in the MTT assay. In spite of this, the particle has advantages such as sustained release or bone targeting function. These advantages have potential allowing the formulation to maintain lower dose and higher anti-cancer efficiency during *in vivo* study.

For MDA-MB-231 cell line, preliminary study showed that the IC₅₀ for both free API and undecorated formulation was around 20 nM. To better illustrate the results and compare the ALE decorated formulation, another study was done using MTT assay with concentration range from 0-50 nM. The results are shown in [Fig. 6-14](#).

Blank particle showed no cytotoxicity, similar to what observed before. On the other hand, all formulation including the free API showed significant anti-cancer effect. Free TPL showed the highest IC₅₀ around 25 nM. For the particle formulations, the undecorated formulation showed slightly enhancement of the performance at 20 nM concentration. However, the IC₅₀ is similar to free API. All ALE decorated formulation indicated better performance than the free drug and undecorated formulation. 4% and 8% ALE NP had IC₅₀ around 20 nM while 6% formulation had as low as 16 nM. This may be influenced by both size and drug releasing differences between three formulations.

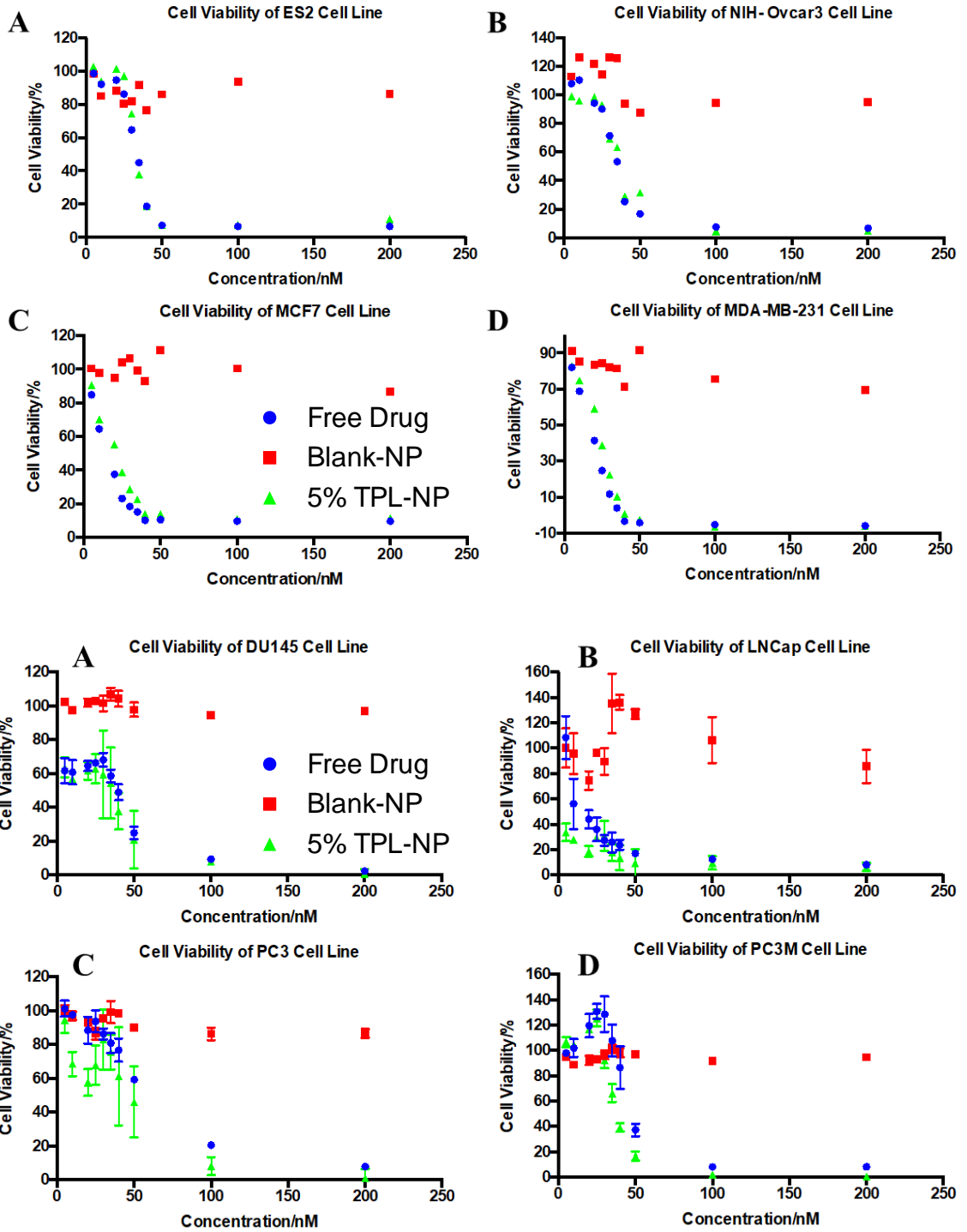


Fig 6-13. MTT results with different cell lines.

Efficacy results for TPL-NP-ALE with MDA-MB-231

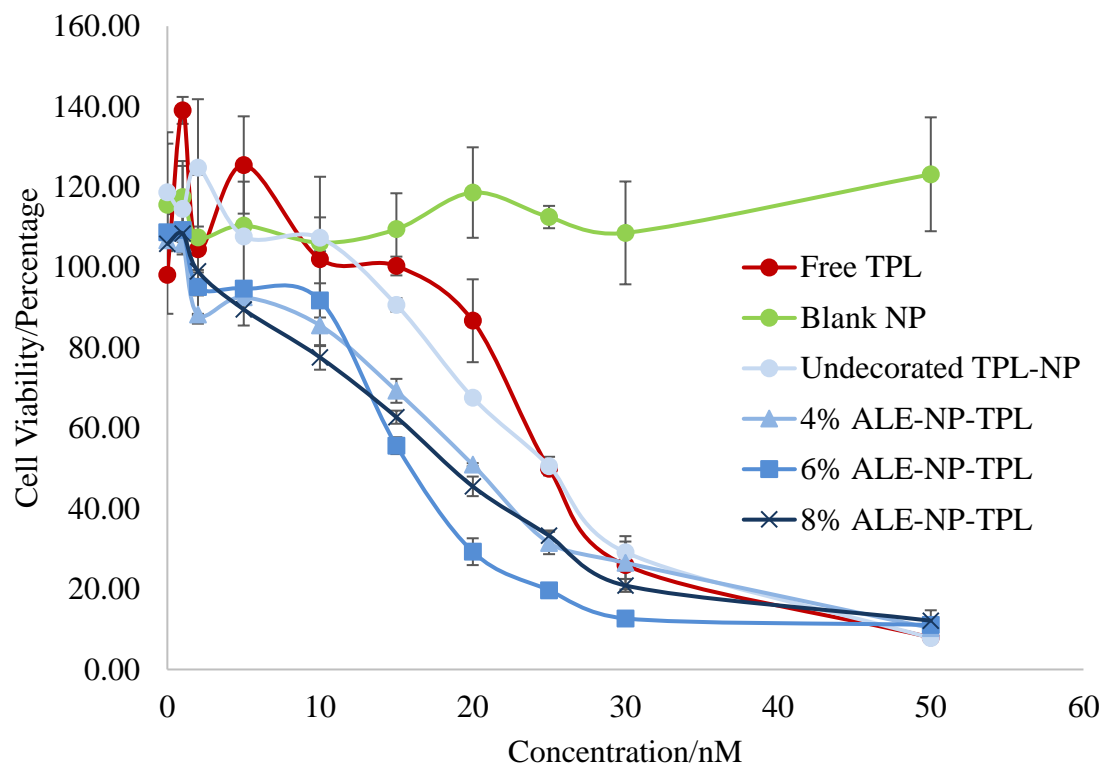


Fig. 6-14. MTT results for different formulations against MDA-MB-231 cell line.

6.2.2. Toxicity study

It is very essential to confirm that TPL or TPL NP are highly potent only to cancer cells. It is challenging if the API is highly toxic to the normal cells. This will make the therapeutic treatment having an extremely narrow therapeutic index, bring in complication to the treatment design. Thus, the toxicity of the formulation was also examined with MC3T3-E1 cell line.

6.2.2.1. MTT assay

MTT assay was used to study the inhibition effect of the treatment to MC3T3-E1 cell lines. The concentration range was set the same as MDA-MB-231 cell lines. Keeping all the condition the same, the results are shown in [Fig. 6-15](#).

The blank particle itself had no toxicity against MC3T3 cells with around 100% cell viability in the concentration range. TPL free drug, on the other hand, has around 40% inhibition rate at concentration higher than 2 nM. All particle formulations showed inhibition effect between blank particle group and the free drug group. General speaking, undecorated particles and 8% ALE-NP-TPL has similar inhibition effect against MC3T3 while 4% and 6% ALE group has slightly higher inhibition effect. This may cause by the particle size different. As shown in [Fig. 6-16](#).

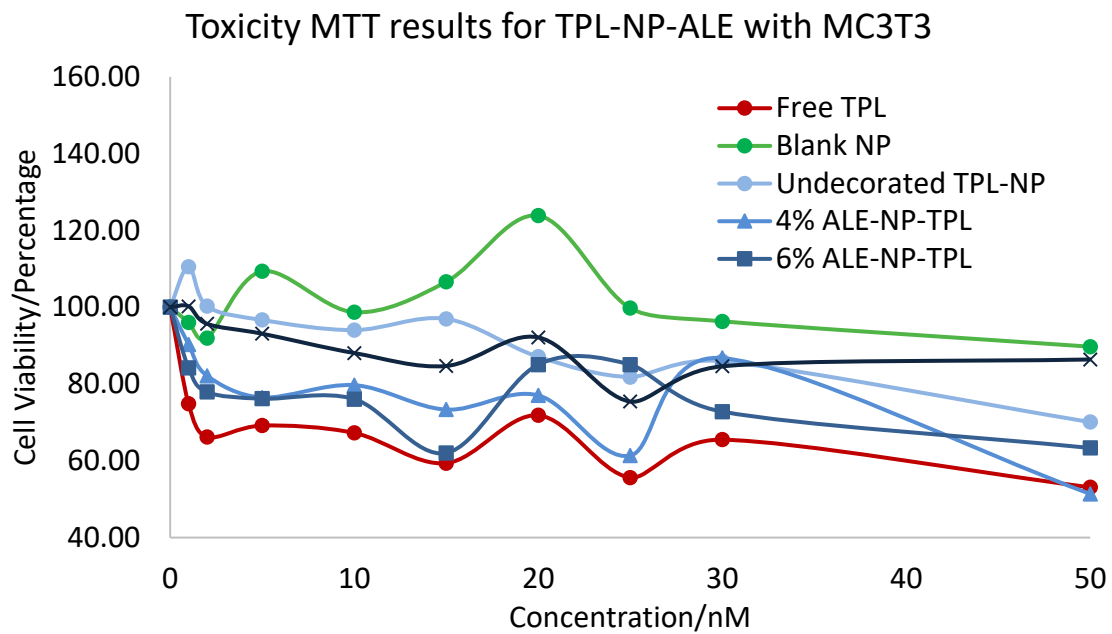


Fig. 6-15. MTT results for toxicity study against MC3T3 cell line.

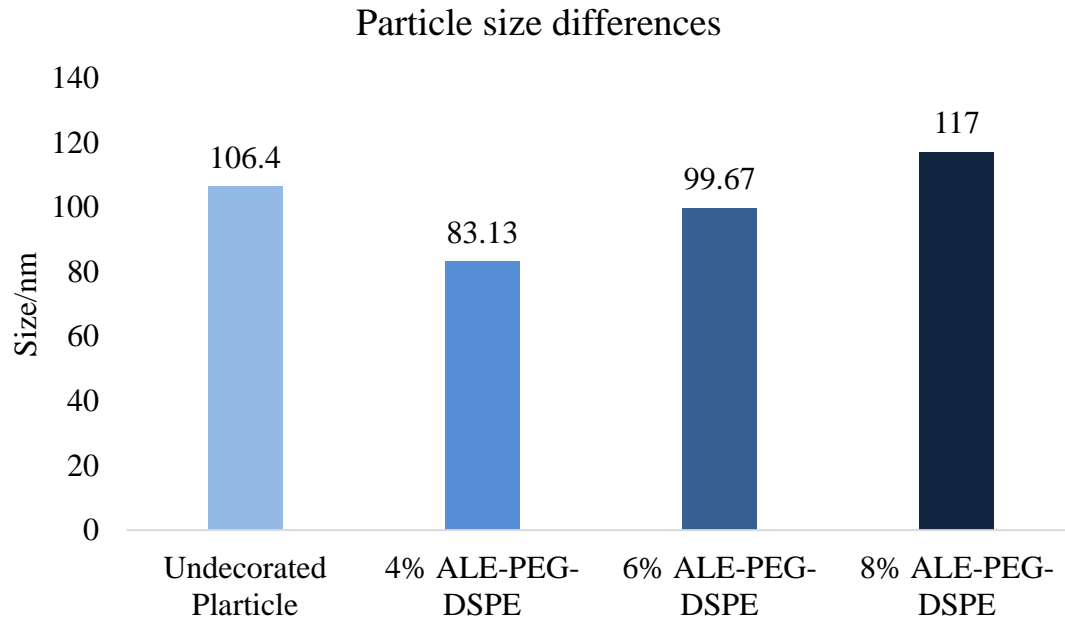


Fig. 6-16. Particle size differences between formulation tested in toxicity study.

6.2.2.2. Clonogenic assay

Although TPL and ALE-NP-TPL have shown growth inhibition against MC3T3-E1 cells, it is not necessary indicating that the treatments are toxic and killing the cells. As mentioned in section 6.5.6., MTT can only reflect the MTT reduction reaction activity, namely the metabolism activity of the cells. Thus, clonogenic assay was also used as a direct measurement of the cell growth and proliferation. The results are shown in Fig. 6-17, 6-18.

As stained by purple color, it was easy to find out that for the treatment group with 6% ALE-NP-TPL at 20 nM, the colonies that formed were significantly less, while all the other groups are comparable with the control group. This result was also illustrated in the graph of colony number (Fig. 7-16). This indicating that with this treatment, not only the metabolism of the cells was inhibited, but the proliferation was also suppressed, suggesting that the treatment is toxic to the cells. Based on this study, 8% ALE-NP-TPL was considered the lowest toxicity to the bone osteoblast. The formulation will be used for future study.

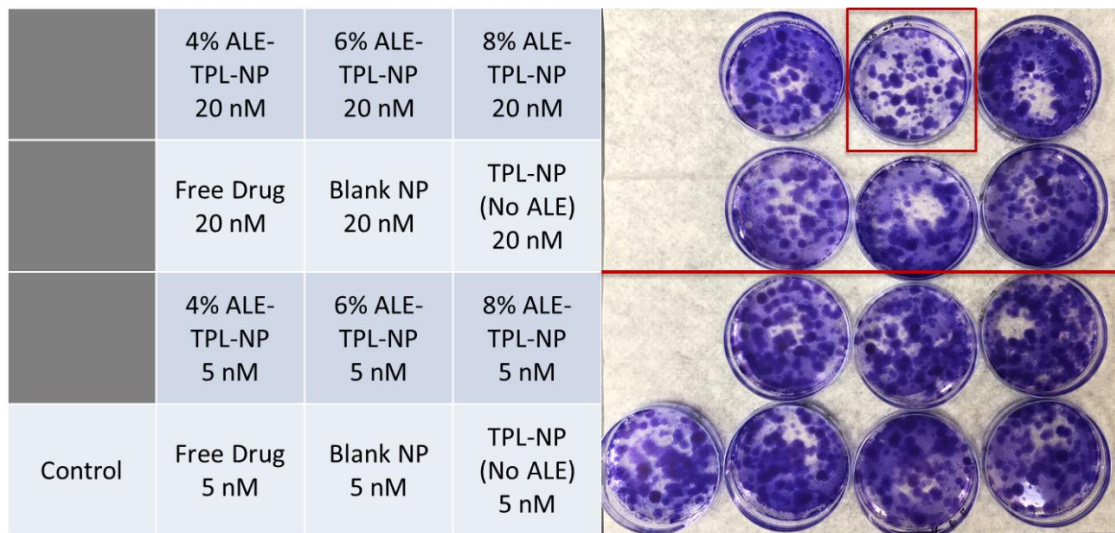


Fig. 6-17. Images of clonogenic assay results.

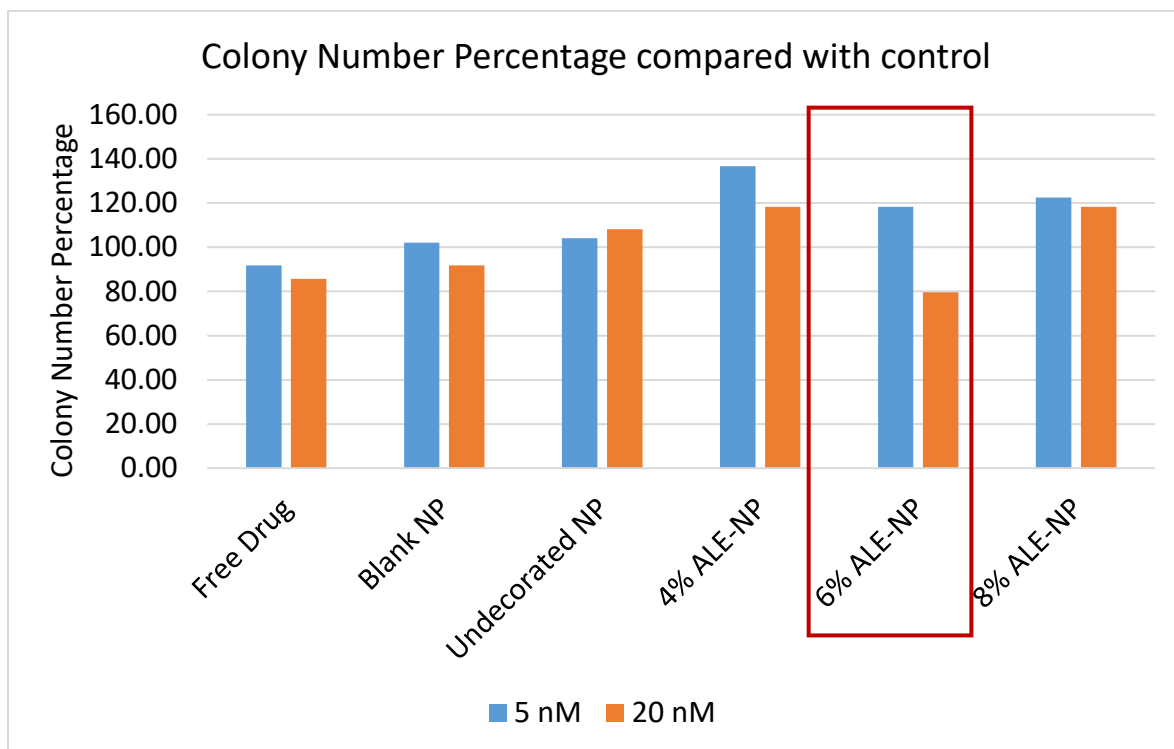


Fig. 6-18. Colony number comparison between different treatment group.

6.2.3. Uptake study

Since the particle treatment will be presented in bone micro environment that both normal cells and cancer cells exist, the uptake of the particles was also studied to compare the differences between different cells. The results are shown in [Fig. 6-19](#).

In the image, blue color represents the cell nucleus while red color represents the particle formulation. Since TPL was highly potent to the MDA-MB-231 cell lines, in order to have strong fluorescence signal, blank particle was used to represent the particle formulation. The dose was set at high concentration of 0.25 mg/mL. It is clearly shown in the images that the MDA-MB-231 cancer cell lines showed significant particle uptake after 4-hour treatment. The red dots (particles) was accumulated around the nucleus inside the cells. On the other hand, MC3T3-E1 cells showed no uptake of the particle. This result benefits our application since it illustrated the minimal influence on the normal bone cells as there was no uptake of the treatment.

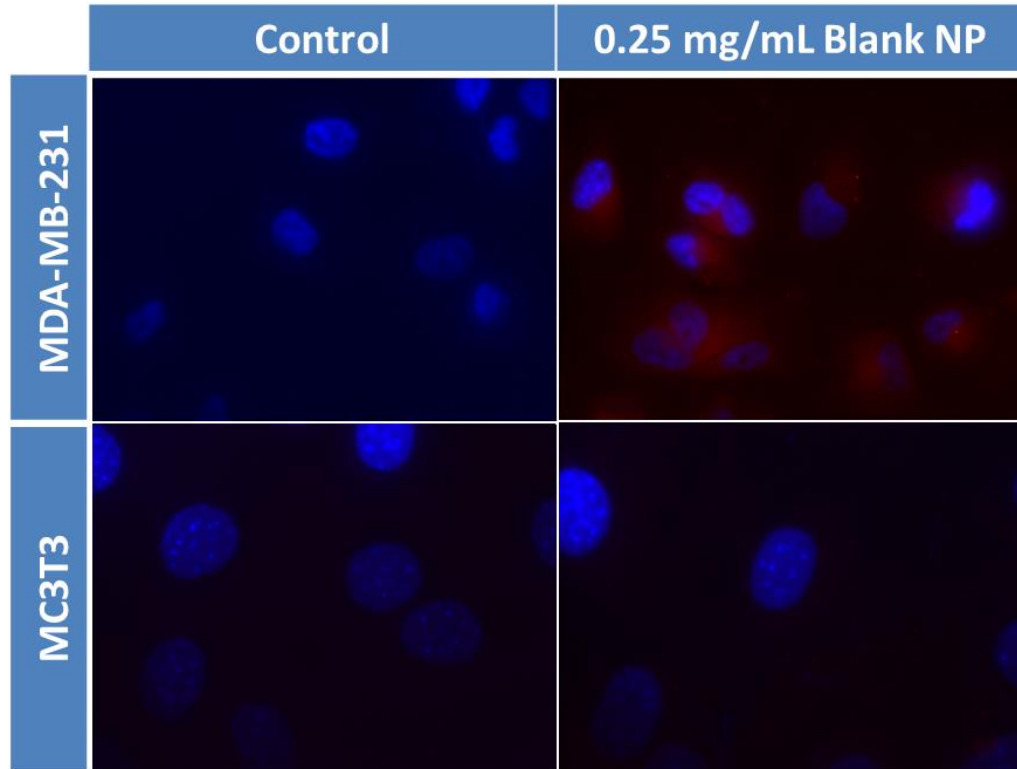


Fig. 6-19. Uptake comparison of MDA-MB-231 and MC3T3 cell lines. Blue color represents the cell nucleus. Red color represents the particle formulation.

6.2.4. Anti-migration test

The anti-migration test was a measurement of how efficient the treatment can stop the cancer cell from migrating. Although the assay cannot separate the influence of migration and proliferation well, it provides a direct view of the purpose. The results are shown in [Fig. 6-20](#).

Without the treatment, PC3M cells showed significant “wound healing” speed. The gap was narrowing up and complete close within 24 hours. On the other hand, with TPL free drug at IC20 concentration treatment, the gap did not change significantly while cell at other places showed normal growth. This result indicated that at low concentration of treatment when the cell cannot be kill sufficiently, the migration of the cancer cell has been inhibited. It emphasized the ability and significance of using the TPL for metastatic cancer treatment.

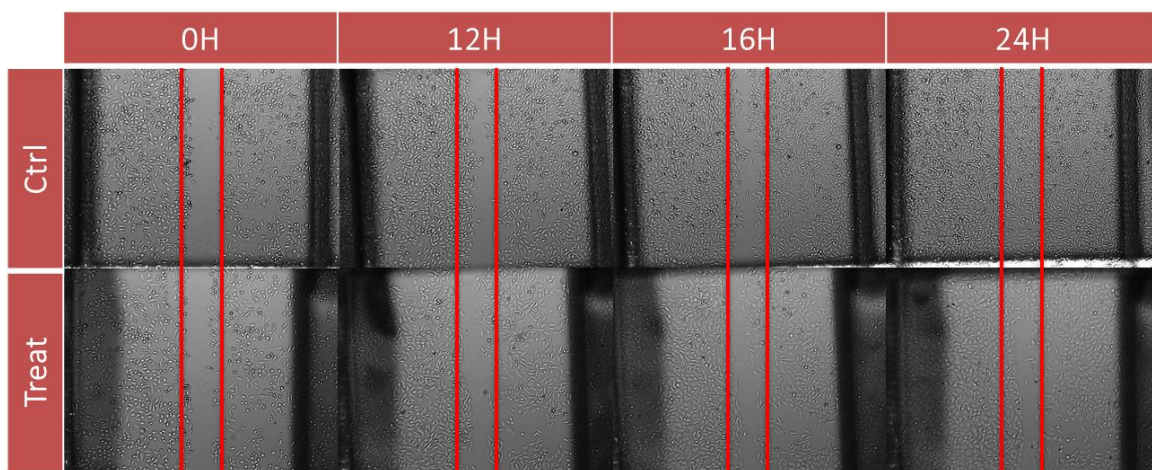


Fig. 6-20. Anti-migration test images.

6.3. Bone binding study

Bone binding efficacy was tested with rats' bone tissue. The results were shown in Fig. 6-21. With the increasing of ALE decorated amount, the fluorescent signal became stronger, indicating more particle binding to the bone. The results agree with the HA binding study showed before. The 8% ALE-NP-TPL formulation showed the best binding efficacy within short period of time, indicating advantages and promising potential in animals or furthermore, in human. With the local injection administration, the formulation may help achieving high local concentration at the metastasis site, accumulating more in breast cancer cells and thus killing the tumor cells.

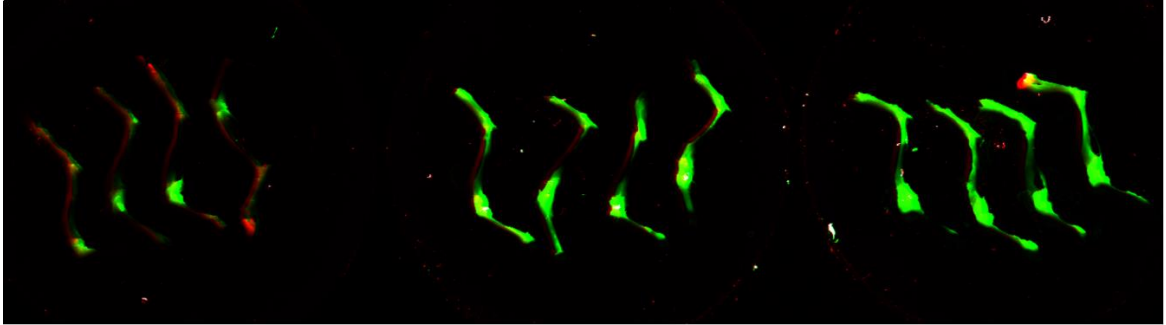


Fig. 6-21. Binding efficacy study with rats' leg bones. From left to right three groups are:
TPL free drug, 4% Alendronate decorated NP with TPL and 8% Alendronate decorated
NP with TPL.

CHAPTER 7. CONCLUSIONS

The particle formulation is essential for not only active ingredients properties, but also determined the biological activity such as uptake, release, biodistribution, pharmacokinetics etc. With the substitution of traditional lipid, triolein oil to DHA, the particle system can not only improve the stability under normal storage condition, but also achieve excellent encapsulation efficiency. Although it has been confirmed that with drug load higher than 5%, the EE significantly dropped, the high potency of the API ensure that the 5% load formulation can achieve efficient therapeutic performance. With the optimization of the formulation, we were able to fabricate TPL encapsulated NP decorated with ALE on the surface. The decorated particles showed significant HA binding efficiency, with a concentration dependent manner. As the HA is the main composite of the bone matrix, the particle delivery systems are highly possible to have high binding efficiency with bone. The sustained releasing of the TPL may prolong the exposure time during *in vivo* study. The ALE decoration also illustrated better formulation stabilization effect that eliminated the burst release effect. The burst release can cause high API exposure with short time, resulting in toxicity. The Cryo-SEM images indicating the particle size distribution of the particle and confirm the hypothesis. Although the administration route of the formulation is *i.m.* injection instead *i.v.*, the particle size still plays important role in particle cell interaction, elimination and toxicity. Final formulation was used as 8% alendronate incorporated nanoparticle with mean size around 100 nm, shown in [Fig. 7-1](#).

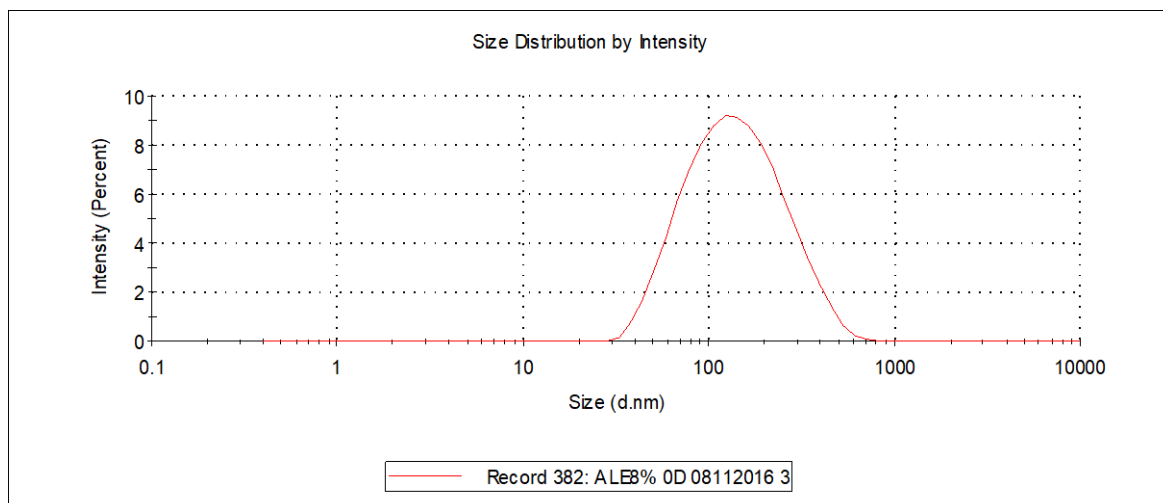


Fig. 7-1. Size distribution (intensity) of 8% ALE-NP-TPL.

In the *in vitro* cell work test, TPL loaded NP showed significant anti-tumor effect against various kinds of cancer. The effective concentration of the treatment was relatively low, which indicated the high potency of the drug. Differences have been observed between different formulation with ALE during breast cancer cell study. These differences may be caused by the size distribution and dissolution variability. Generally speaking, nanoparticle formulations with ALE have enhanced the anti-cancer effect compared with TPL free drug. The particle may be able to elevate the uptake of the TPL, and sustained release the drug molecule so that the concentration in the cells can stay longer above the therapeutic dose. On the other hand, 6% ALE-NP-TPL showed toxic

against normal bone cells MC3T3-E1 during clonogenic assay. The results illustrated that the specific formulation might inhibit both metabolism and proliferation of the cell. On the other hand, 8% ALE-NP-TPL not only showed higher affinity, but also low toxicity compared with other formulation.

Since the formulation will be delivered into the bone microenvironment where both cancer cell and normal bone cell exists, uptake study showed the different uptake behavior of the cells to the formulation. It has been discovered that cancer cells showed significant uptake compared to normal bone cell at the same condition. This may due to the fact that smaller size of cancer cells promoting the interaction between the cell membrane and the particle formulation, resulting in more endocytosis and more uptake. The results benefit the hypothesis of the study to achieve anti-cancer effect while stay low toxicity to normal cells.

The preliminary *in vivo* results also showed the tumor inhibition in mice. With each *i.v.* injection, the tumor stopped growing, or even shrink after the treatment. In order to minimize the toxicity of TPL, local injection of the formulation was used as a new administrative route. The pharmacokinetic study was down with rats to evaluate the targeting efficacy of the formulation.

REFERENCE LIST

[Cancer Statistics, 2017] CA Cancer J Clin. 2017 Jan;67(1):7-30. doi:

10.3322/caac.21387. Epub 2017 Jan 5.

[Breast cancer, 2018] <https://breast-cancer.ca/metsurv-stat/>

[Breast Cancer Metastasis, 2016] <http://healthandsymptoms.com/cancer/breast-cancer/understanding-breast-cancer-metastasis/>

[Dai, Xiaofeng, 2017] Dai, Xiaofeng, et al. "Breast cancer cell line classification and its relevance with breast tumor subtyping." Journal of Cancer 8.16 (2017): 3131.

[Scully O J, 2012] Scully O J, Bay B H, Yip G, et al. Breast cancer metastasis[J]. Cancer Genomics-Proteomics, 2012, 9(5): 311-320.

[Parkes, Amanda, 2018] Parkes, Amanda, et al. "Characterization of bone only metastasis patients with respect to tumor subtypes." NPJ breast cancer 4.1 (2018): 2.

[Manders, Klaartje, 2006] Manders, Klaartje, et al. "Clinical management of women with metastatic breast cancer: a descriptive study according to age group." BMC cancer 6.1 (2006): 179.

[Coleman R E, 1987] Coleman R E, Rubens R D. The clinical course of bone metastases from breast cancer[J]. British journal of cancer, 1987, 55(1): 61.

[Chen, Yu-Chi, 2010] Chen, Yu-Chi, Donna M. Sosnoski, and Andrea M. Mastro. "Breast cancer metastasis to the bone: mechanisms of bone loss." Breast cancer research 12.6 (2010): 215.

[Liu, Zi, 2011] Liu, Zi, Liang Ma, and Guang-Biao Zhou. "The main anticancer bullets of the Chinese medicinal herb, thunder god vine." *Molecules* 16, no. 6 (2011): 5283-5297.

[Li, Di-Cai, 2009] Li, Di-Cai, Xian-Ke Zhong, Zhi-Ping Zeng, Jian-Guo Jiang, Lin Li, Mou-Ming Zhao, Xiao-Quan Yang et al. "Application of targeted drug delivery system in Chinese medicine." *Journal of Controlled Release* 138, no. 2 (2009): 103-112.

[Zhou Z L, 2012] Zhou Z L, Yang Y X, Ding J, et al. Triptolide: structural modifications, structure–activity relationships, bioactivities, clinical development and mechanisms[J]. *Natural product reports*, 2012, 29(4): 457-475.

[Westfall, Suzanne D, 2007] Westfall, Suzanne D., Eric E. Nilsson, and Michael K. Skinner. "Role of triptolide as an adjunct chemotherapy for ovarian cancer." *Chemotherapy* 54, no. 1 (2007): 67-76.

[Phillips, Phoebe A., 2007] Phillips, Phoebe A., d, and Ashok K. Saluja. "Triptolide induces pancreatic cancer cell death via inhibition of heat shock protein 70." *Cancer research* 67, no. 19 (2007): 9407-9416.

[YinJun, Lou, 2005] YinJun, Lou, Jin Jie, and Wang YunGui. "Triptolide inhibits transcription factor NF-kappaB and induces apoptosis of multiple myeloma cells." *Leukemia research* 29, no. 1 (2005): 99-105.

[Carter, Bing Z, 2008] Carter, Bing Z., Duncan H. Mak, Wendy D. Schober, Martin F. Dietrich, Clemencia Pinilla, Lyubomir T. Vassilev, John C. Reed, and Michael Andreeff. "Triptolide sensitizes AML cells to TRAIL-induced apoptosis via decrease of XIAP and p53-mediated increase of DR5." *Blood* 111, no. 7 (2008): 3742-3750.

[Shi, Xianping, 2009] Shi, Xianping, Yanli Jin, Chao Cheng, Hui Zhang, Waiyi Zou, Qin Zheng, Zhongzheng Lu, Qi Chen, Yingrong Lai, and Jingxuan Pan. "Triptolide inhibits Bcr-Abl transcription and induces apoptosis in STI571-resistant chronic myelogenous leukemia cells harboring T315I mutation." *Clinical Cancer Research* 15, no. 5 (2009): 1686-1697.

[Lin, J., 2007] Lin, J., L. Y. Chen, Z. X. Lin, and M. L. Zhao. "The effect of triptolide on apoptosis of glioblastoma multiforme (GBM) cells." *Journal of International Medical Research* 35, no. 5 (2007): 637-643.

[Wang, Zhipeng, 2009] Wang, Zhipeng, Haifeng Jin, Ruodan Xu, Qibing Mei, and Daiming Fan. "Triptolide downregulates Rac1 and the JAK/STAT3 pathway and inhibits colitis-related colon cancer progression." *Experimental & molecular medicine* 41, no. 10 (2009): 717-727.

[Huang, Weiwei, 2012] Huang, Weiwei, Tiantian He, Chengsen Chai, Yuan Yang, Yahong Zheng, Pei Zhou, Xiaoxia Qiao et al. "Triptolide inhibits the proliferation of prostate cancer cells and down-regulates SUMO-specific protease 1 expression." *PloS one* 7, no. 5 (2012): e37693.

[Lu, L. H., 1992] Lu, L. H., Lian, Y. Y., He, G. Y., Lin, S. P., Huan, S. H., Chen, Z. Z., Dend, H. X., and Zheng, Y. L. Clinical study of triptolide in treatment of acute leukemia. *Clin. Exp. Investig. Hematol.*, 3: 1-3, 1992.

[Park B, 2014] Park B. Triptolide, a diterpene, inhibits osteoclastogenesis, induced by RANKL signaling and human cancer cells[J]. *Biochimie*, 2014, 105: 129-136.

[Chugh, Rohit, 2012] Chugh, Rohit, Veena Sangwan, Satish P. Patil, Vikas Dudeja, Rajinder K. Dawra, Sulagna Banerjee, Robert J. Schumacher et al. "A preclinical evaluation of Minnelide as a therapeutic agent against pancreatic cancer." *Science translational medicine* 4, no. 156 (2012): 156ra139-156ra139.

[Narvekar, Mayuri, 2014] Narvekar, Mayuri, Hui Yi Xue, June Young Eoh, and Ho Lun Wong. "Nanocarrier for poorly water-soluble anticancer drugs—barriers of translation and solutions." *AAPS PharmSciTech* 15, no. 4 (2014): 822-833.

[Hermanson G T, 2013] Hermanson G T. *Bioconjugate techniques*[M]. Academic press, 2013.

[Yang S, 2003] Yang S, Chen J, Guo Z, et al. Triptolide inhibits the growth and metastasis of solid tumors1[J]. *Molecular cancer therapeutics*, 2003, 2(1): 65-72.

[Galletti, Elena, 2007] Galletti E, Magnani M, Renzulli M L, et al. Paclitaxel and docetaxel resistance: molecular mechanisms and development of new generation taxanes[J]. *ChemMedChem*, 2007, 2(7): 920-942.

[Guo, Qingpeng, 2013] Guo Q, Nan X X, Yang J R, et al. Triptolide inhibits the multidrug resistance in prostate cancer cells via the downregulation of MDR1 expression[J]. *Neoplasma*, 2013, 60(6): 598-604.

[Chen Y W, 2010] Chen Y W, Lin G J, Chuang Y P, et al. Triptolide circumvents drug-resistant effect and enhances 5-fluorouracil antitumor effect on KB cells[J]. *Anti-cancer drugs*, 2010, 21(5): 502-513.

[Park B, 2014] Park B. Triptolide, a diterpene, inhibits osteoclastogenesis, induced by RANKL signaling and human cancer cells[J]. *Biochimie*, 2014, 105: 129-136.

[Shao F, 2007] Shao F, Wang G, Xie H, et al. Pharmacokinetic study of triptolide, a constituent of immunosuppressive chinese herb medicine, in rats[J]. *Biological and Pharmaceutical Bulletin*, 2007, 30(4): 702-707.

[Chi-hin, Cho, 2017] Chi-hin, Cho, ed. *Therapeutic Targets for Inflammation and Cancer: Novel Therapies for Digestive Diseases*. World Scientific, 2017.

[Peracchia M T, 1999] Peracchia M T, Fattal E, Desmaele D, et al. Stealth® PEGylated polycyanoacrylate nanoparticles for intravenous administration and splenic targeting[J]. *Journal of Controlled Release*, 1999, 60(1): 121-128.

[Boanini E, 2008] Boanini E, Torricelli P, Gazzano M, et al. Alendronate–hydroxyapatite nanocomposites and their interaction with osteoclasts and osteoblast-like cells[J]. *Biomaterials*, 2008, 29(7): 790-796.

[Riss TL, 2013] Riss TL, Moravec RA, Niles AL, et al. *Cell Viability Assays* [Internet]. Bethesda (MD): Eli Lilly & Company and the National Center for Advancing Translational Sciences 2013 May 1.

[Liu P, 2015] Liu P, Sun L, Zhou D, et al. Development of alendronate-conjugated poly (lactic-co-glycolic acid)-dextran nanoparticles for active targeting of cisplatin in osteosarcoma[J]. *Scientific reports*, 2015, 5: 17387.

[Zhang C, 2014] Zhang C, Peng F, Liu W, et al. Nanostructured lipid carriers as a novel oral delivery system for triptolide: induced changes in pharmacokinetics profile

associated with reduced toxicity in male rats[J]. International journal of nanomedicine, 2014, 9: 1049.

[Roodman G D., 2004] Roodman G D. Mechanisms of bone metastasis[J]. New England Journal of Medicine, 2004, 350(16): 1655-1664.

[Gulati N, 2011] Gulati N, Gupta H. Parenteral drug delivery: a review[J]. Recent patents on drug delivery & formulation, 2011, 5(2): 133-145.

[About Cancer] <http://www.aboutcancer.com/bre4b.htm>